

Application of Overset Grid Methodology to Micro Rotor Simulations

Vinod K. Lakshminarayan
Research Associate

James D. Baeder
Associate Professor

*Alfred Gessow Rotorcraft Center
University of Maryland*



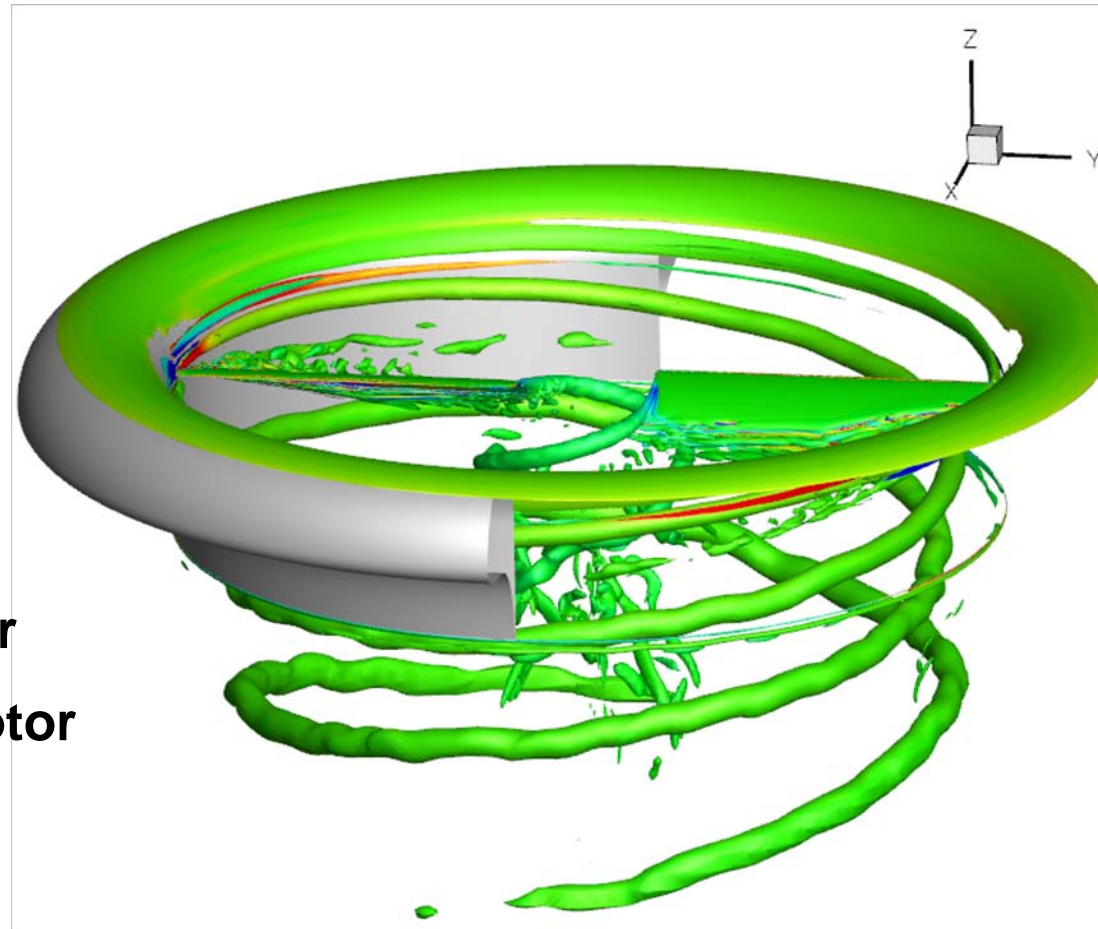
Symposium on Overset Composite Grids and Solution Technology
September 20-23, 2010, Moffett Field, California



Outline



- Introduction
- Methodology
- Results
 - Micro-Scale Single Rotor
 - Out of ground effect
 - In ground effect
 - Micro-Scale Coaxial Rotor
 - Micro-Scale Shrouded Rotor
- Summary

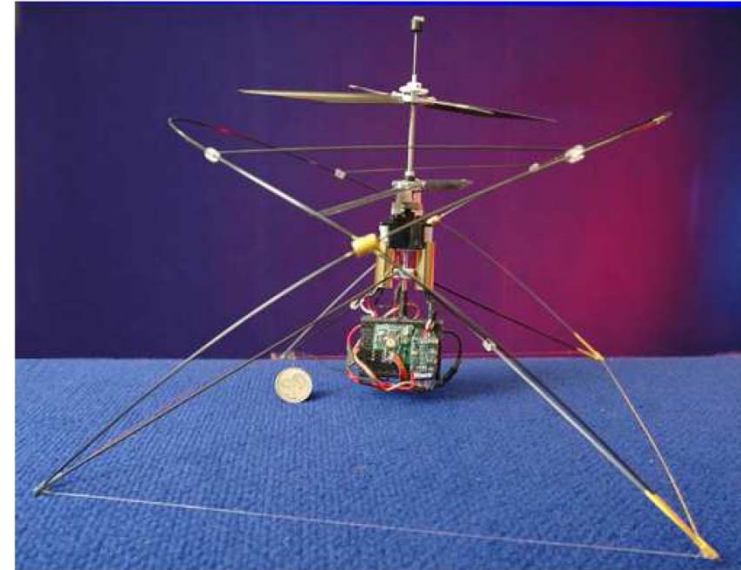




Micro Air Vehicles



- **Micro Air Vehicles (MAVs) as defined by DARPA**
 - ➔ Dimension < 6 inches
 - ➔ Weight < 100g
 - ➔ Endurance > 1 hour
- **Can be used for variety of civilian and military operations**
- **Most current day MAVs lack capabilities demanded by various operations**
- **Apart from aerodynamic improvements, variety of unconventional configurations being studied**
 - ➔ Coaxial rotor, Shrouded rotor, Cycloidal rotor etc.



University of Maryland Micor

Overset methodology make it feasible to study complex geometries



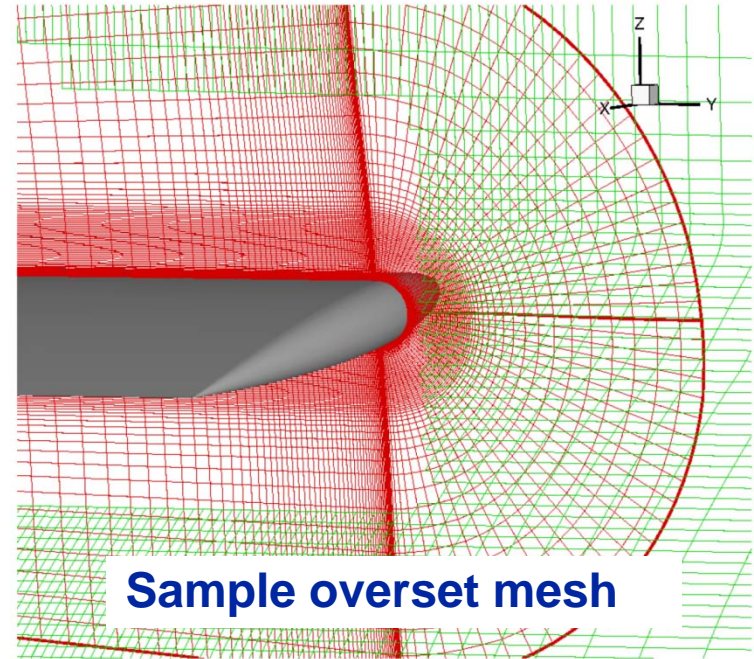
Overset Methodology



- Ability to use fine smoothly spaced meshes in regions of interest
- Involves:
 - Identifying overlap regions
 - Generate connectivity information
 - Exchange information across meshes at every time-step
- Issues:
 - Additional work
 - Loss of conservation property and accuracy
 - Minimized if mesh sizes are similar in interpolation region

Traditional Methodology

- 'Hole-cut' in regions of solid surface
 - Hole points blanked to avoid contamination
- Holes expanded to find optimum hole



Hole points → iblack = 0

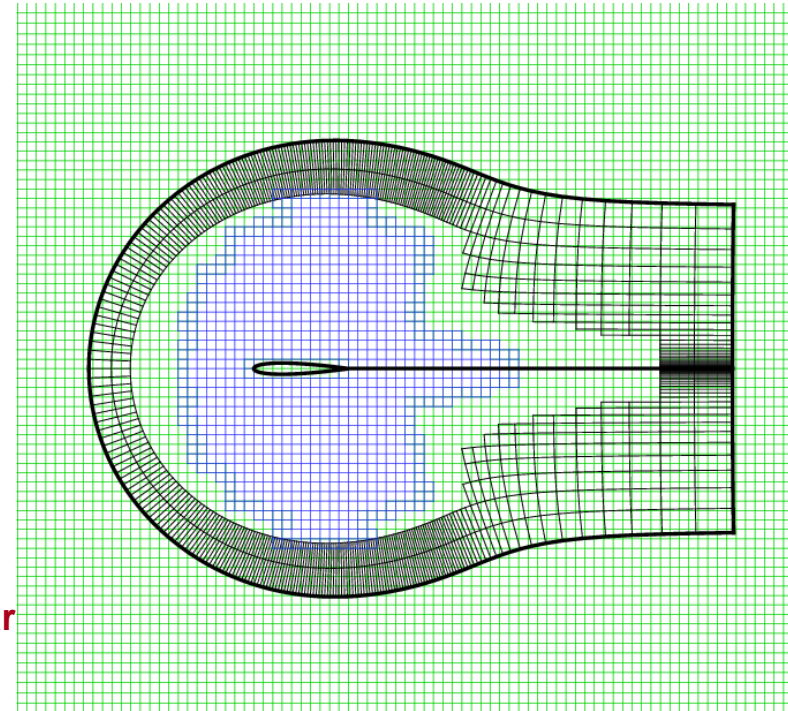
Field points → iblack = 1

Fringe points → iblack = 0 or 1



Implicit Hole-Cutting Method

- Alternative approach developed by Lee & Baeder, 2008
- Why is it called Implicit Hole-cutting?
 - No explicit hole involved (**no hole points**)
 - Points are either field or fringe points
 - Based on cell volume comparison
 - Solution obtained on mesh with smallest cell volume and interpolated to overlapping meshes
 - Presence of hole felt by mesh refinement
 - E.g. Blade mesh points chosen as field point near blade surface due to near-wall refinement
 - Interpolation region is implicitly optimum
- No iblanking involved
- Larger number of fringe points compared to traditional method



- Blue: Fringe points in background mesh
- Black: Fringe points in airfoil mesh
- Green: Field points in background mesh

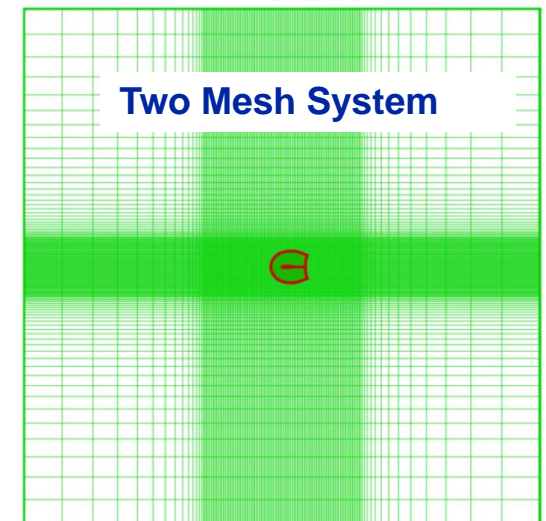
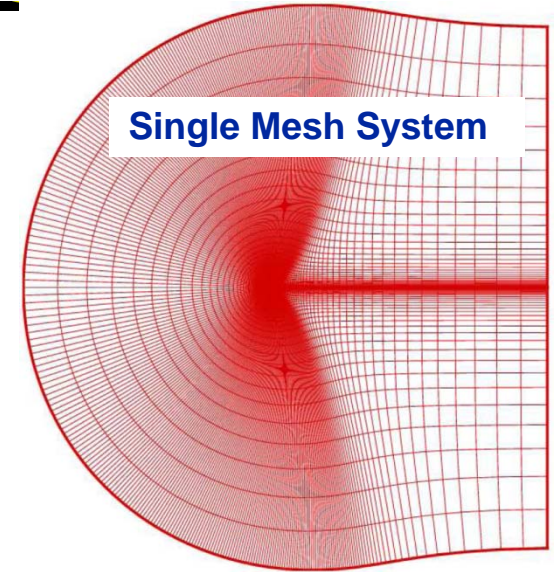
Connectivity done using IHC



Validation of IHC

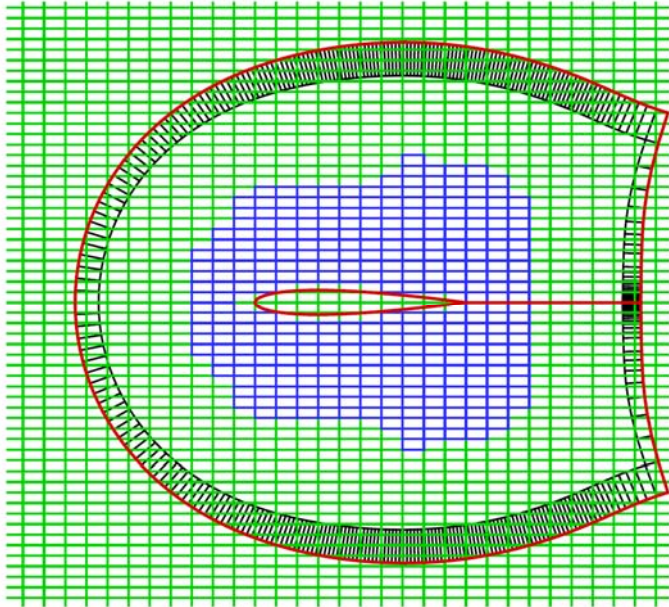


- **Steady 2D flow**
 - NACA 0012 airfoil
 - Angle of attack → 10°
 - Mach Number → 0.3
 - Reynolds Number → 3×10^6
- **Modeled with**
 - Single mesh (327 X 85)
 - Two mesh
 - Airfoil mesh (267 X 65)
 - Background mesh (151 X 151)
 - Connectivity using implicit hole-cutting



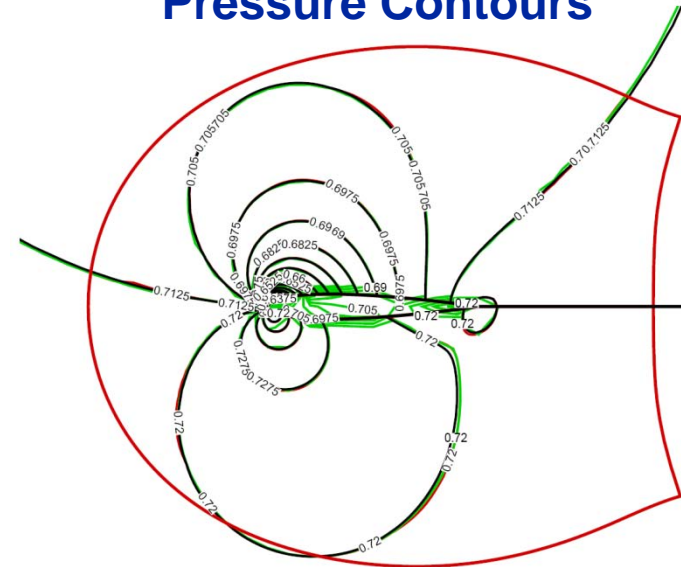


Baseline Implicit Hole-Cutting



- Blue: Fringe points in background mesh
- Black: Fringe points in airfoil mesh
- Green: Field points in background mesh

Pressure Contours

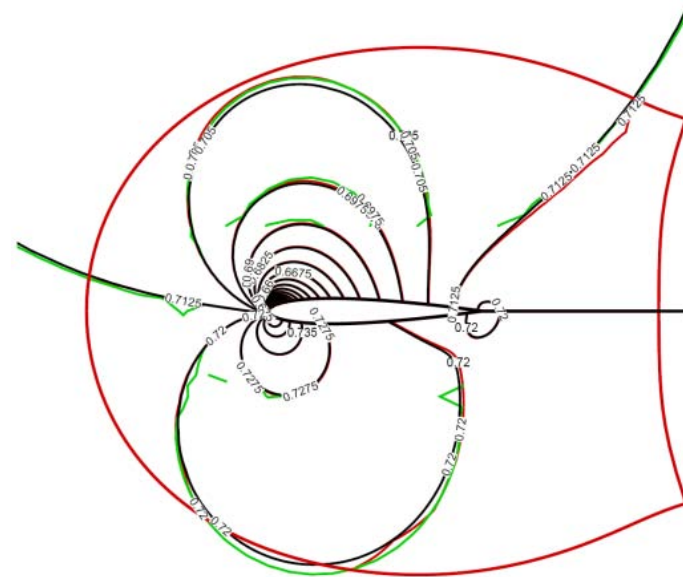
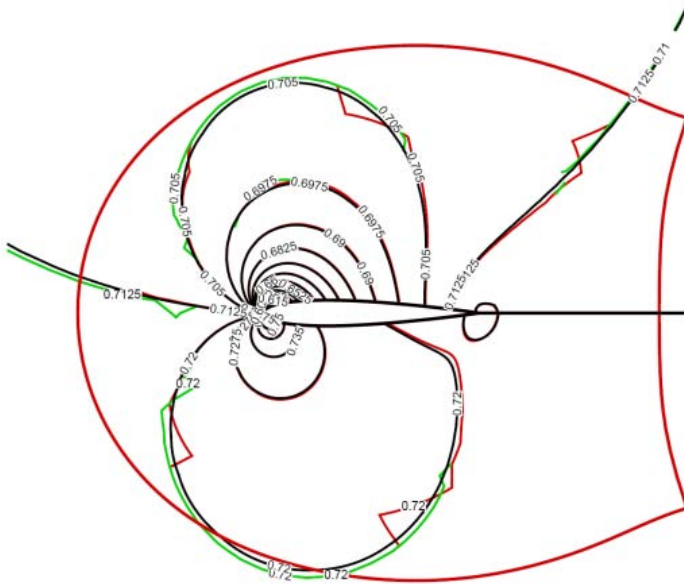


- Black: Contours on single mesh
- Red: Contours on airfoil mesh
- Green: Contours on background mesh

Contours fairly comparable

Issues with baseline IHC

- ➔ Requires thick fringe layers to prevent contamination from invalid points
 - ➔ Not guaranteed in all circumstances
 - ➔ Increased communication time for parallel computation in 3D



- **Improves solution**
- **Inaccuracies and discontinuity still present**
 - **Applicable to even baseline hole-cutting methodology**



Improved Iblanking



- **Inconsistency in the treatment of fringe points**
- **Solution at fringe points are valid**
 - Should be utilized for calculating fluxes
 - Suggests $iblack = 1$ for the RHS of the solver
- **Updates at fringe points invalid during implicit inversion**
 - Can result in contamination
 - Suggest $iblack = 0$ for the LHS of the solver
- **Define $iblack = -1$ for fringe points**
- **Use $abs(iblack)$ in the RHS**
- **Use $max(iblack, 0)$ in the LHS**



Results from Micro-Rotor Simulations





Flow Solver Methodology



OVERTURNS: Compressible overset structured RANS solver

- **Standard discretization**
 - ➔ Inviscid terms: 3rd order MUSCL scheme utilizing Koren's limiter, Roe's flux difference
 - ➔ Viscous terms: 2nd order central
- **Time-accurate computation using preconditioned dual-time scheme in diagonalized approximate factorization framework**
 - ➔ Implicit approximate factorization developed by Pulliam and Chaussee
 - ➔ Turkel Preconditioning for Low Mach numbers
- **Spalart-Allmaras turbulence model with rotational correction**
- **Point-sink boundary condition at far-field boundaries**
- **Connectivity using Implicit Hole cutting (IHC) technique**



Micro-Scale Single Rotor



Hovering Micro-Rotor



2-bladed rotor setup of Ramasamy et al.

- Untwisted rectangular
- Aspect Ratio of 4.39

Airfoil profile

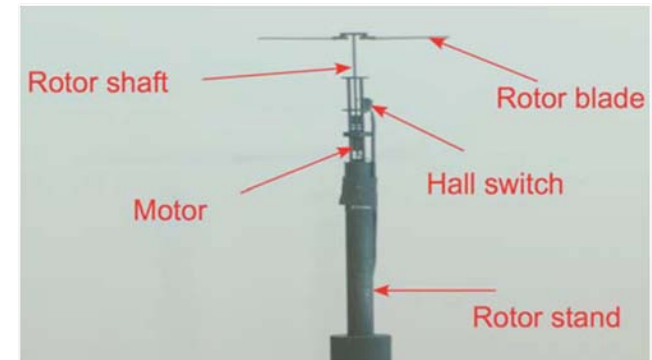
- Circular arc
- 3.7% Thickness
- 3.3% Camber

Flow conditions

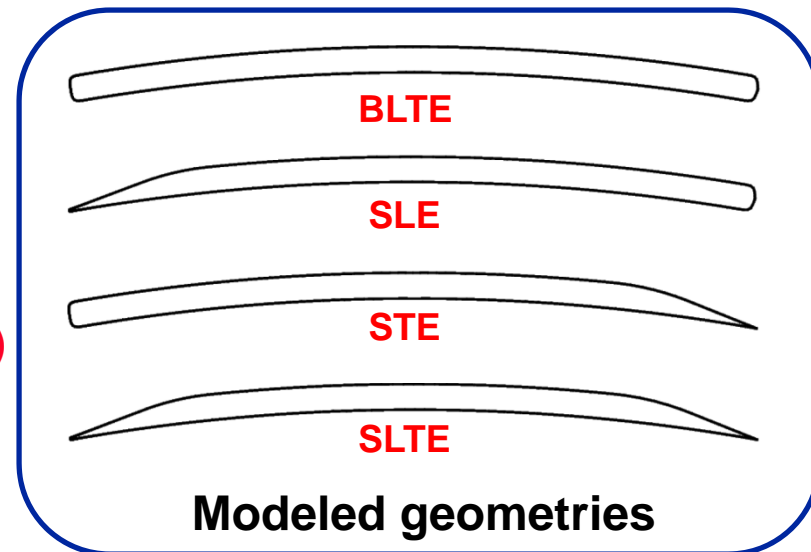
- $Re_{tip} = 32,400$, $Re_{root} = 6480$
- $M_{tip} = 0.08$

Modeled geometry has:

1. Blunt LE and blunt TE (**baseline/BLTE**)
2. Sharp LE and blunt TE (**SLE**)
3. Blunt LE and sharp TE (**STE**)
4. Sharp LE and sharp TE (**SLTE**)



Experimental setup
Ramasamy et al.

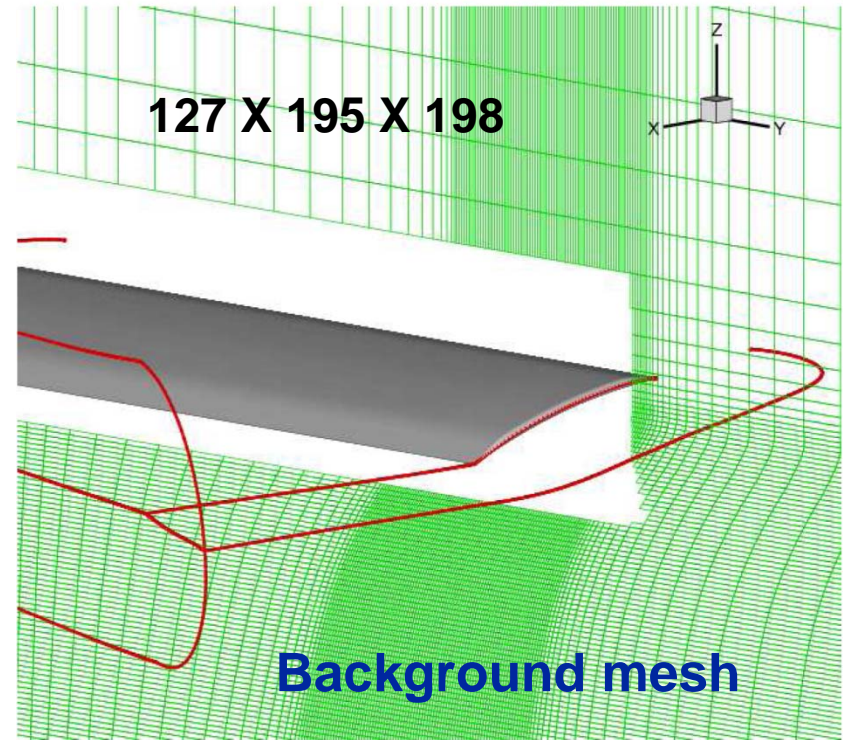
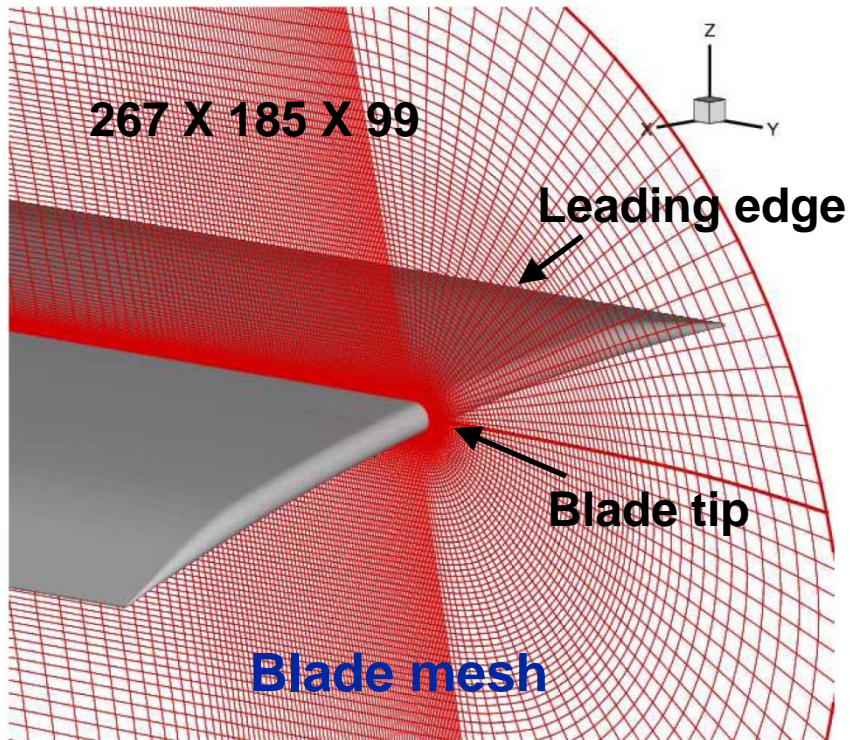


Modeled geometries



Mesh System – Fine

(12° collective setting – SLTE geometry)

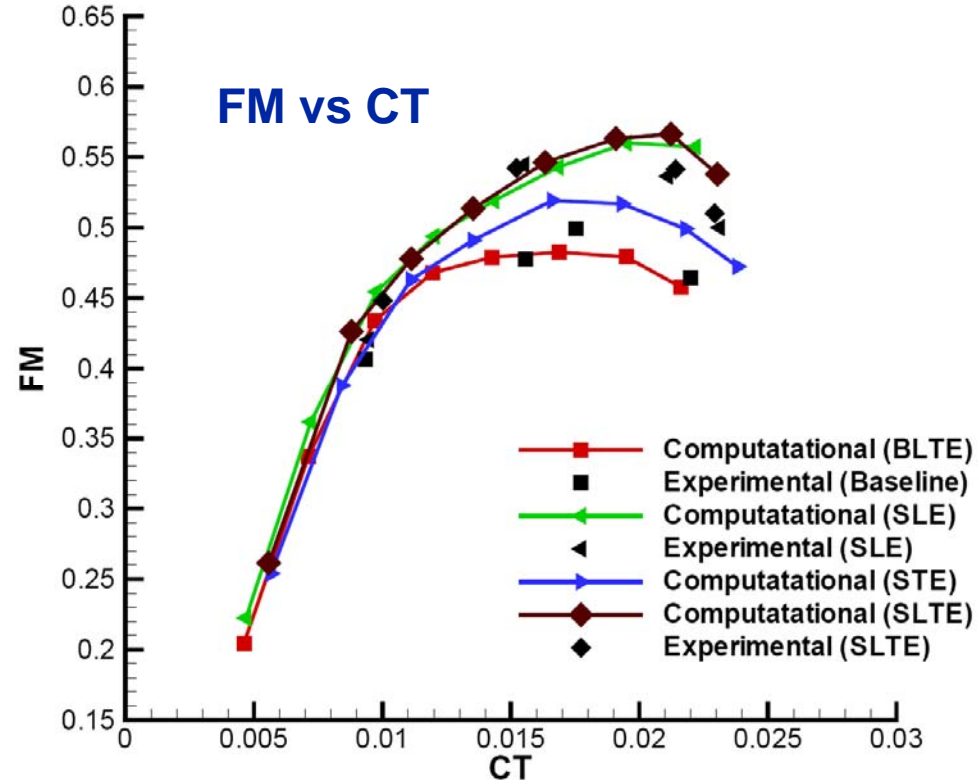
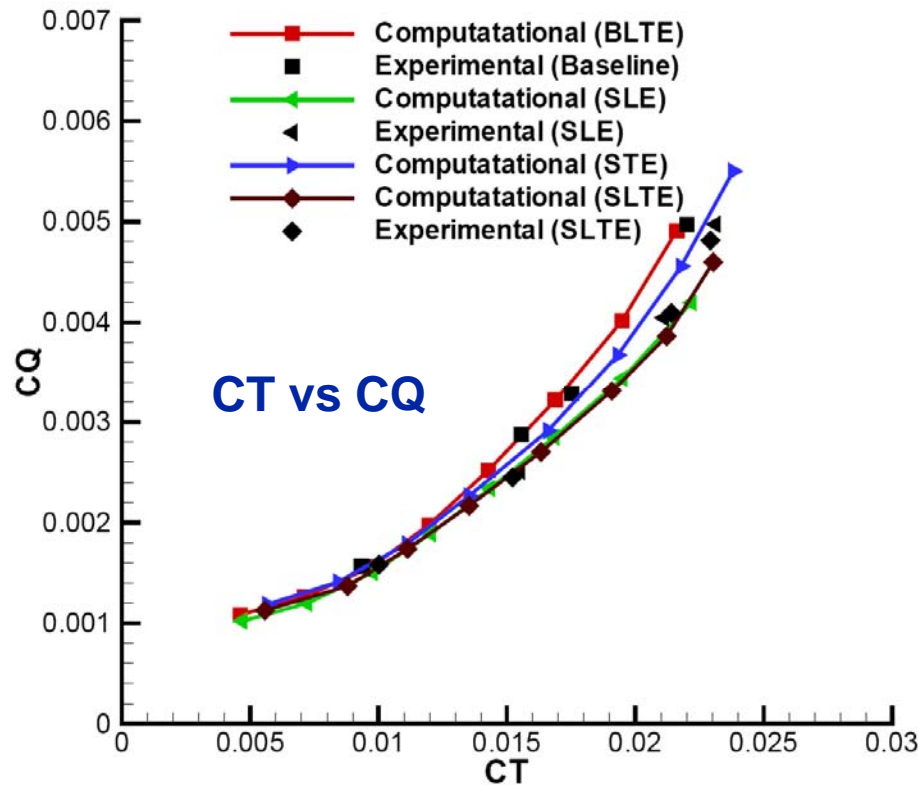


- Total mesh points ~ 10 million
- In most refined regions
 - $\Delta r = 0.02$ chords, $\Delta z = 0.02$ chords, $\Delta \psi = 1.5^\circ$, background

Coarser mesh used for performance comparison



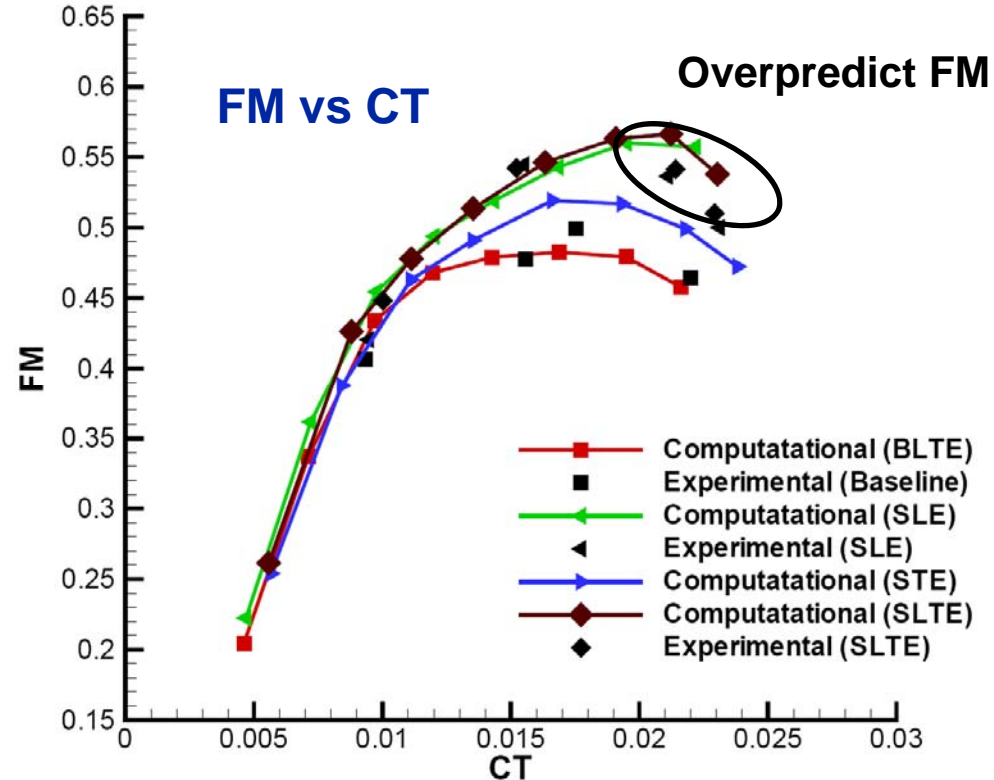
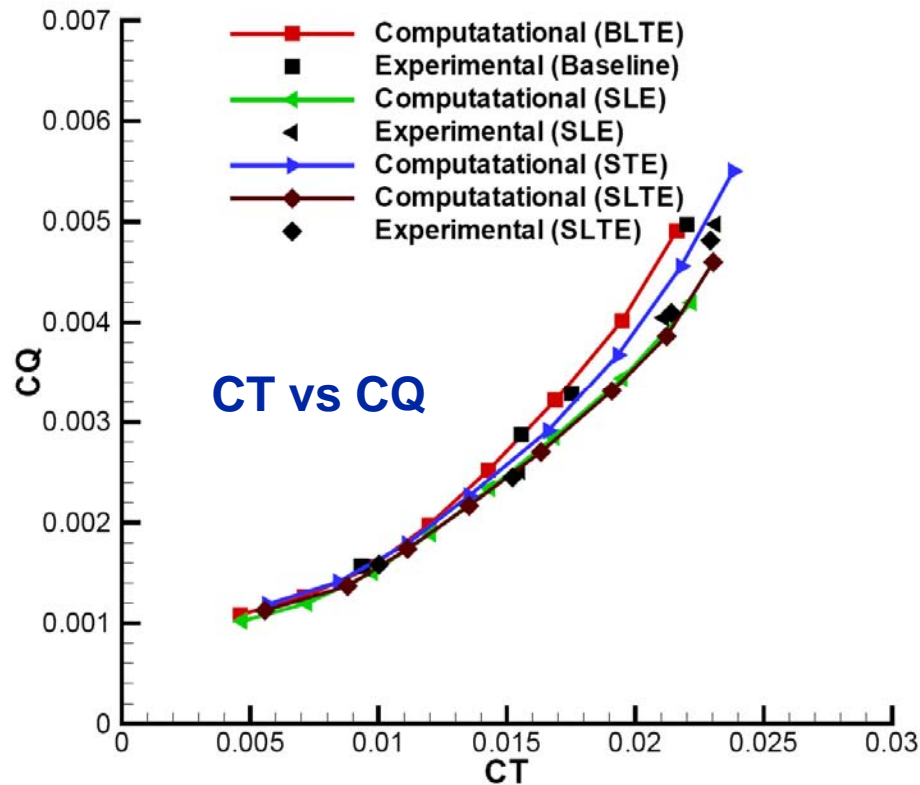
Performance Comparison



Reasonably good comparison between CFD and experiment



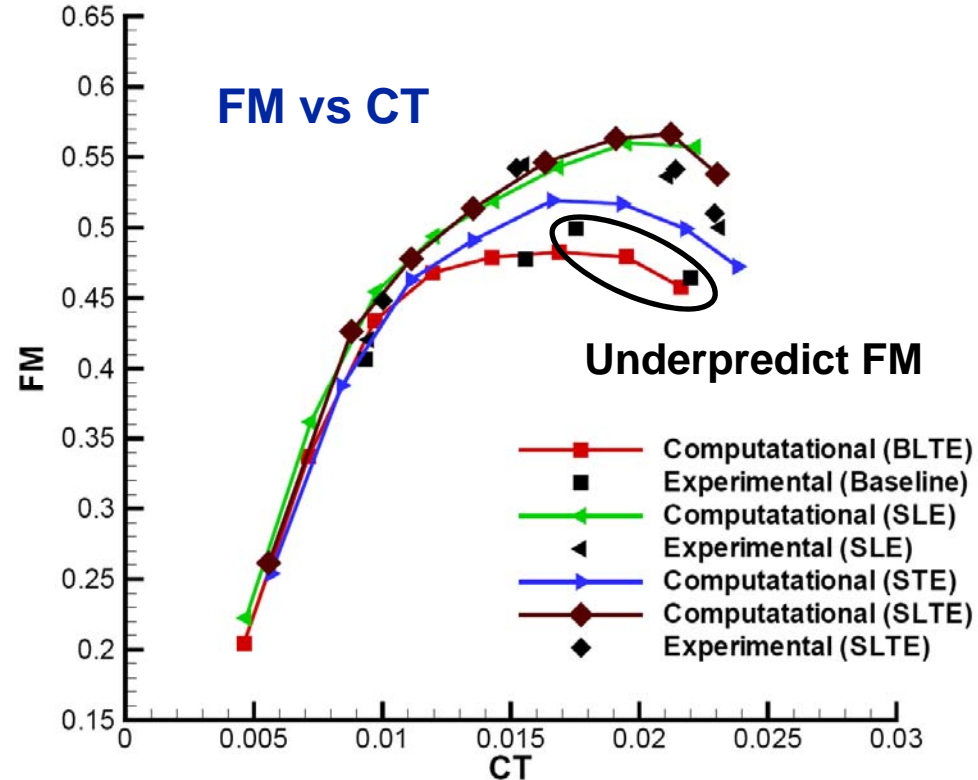
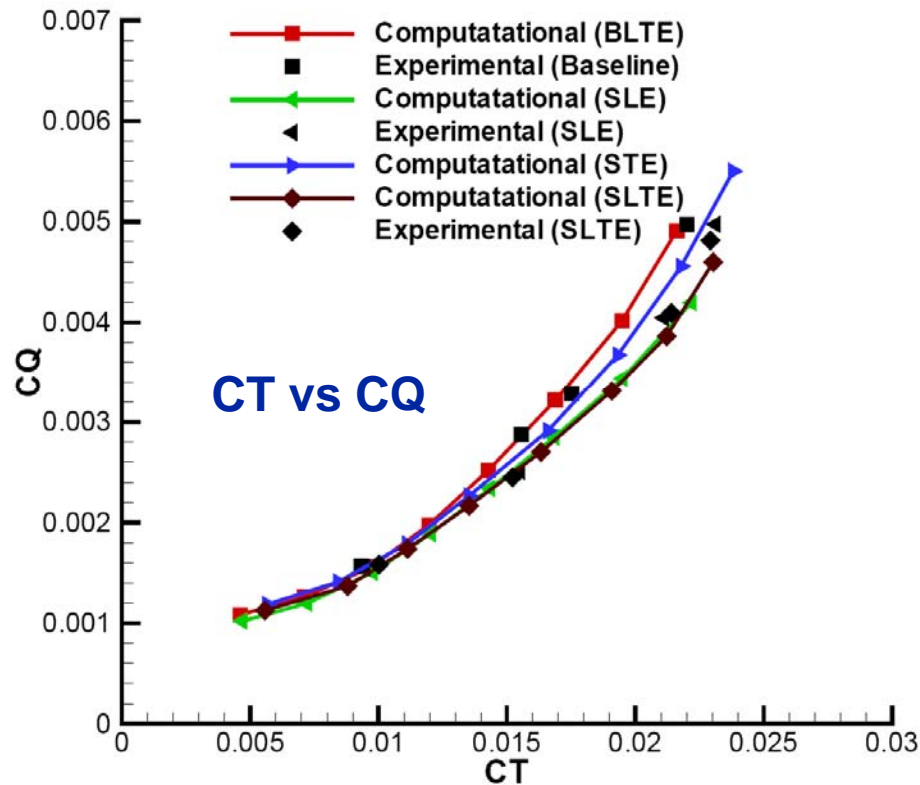
Performance Comparison



Reasonably good comparison between CFD and experiment



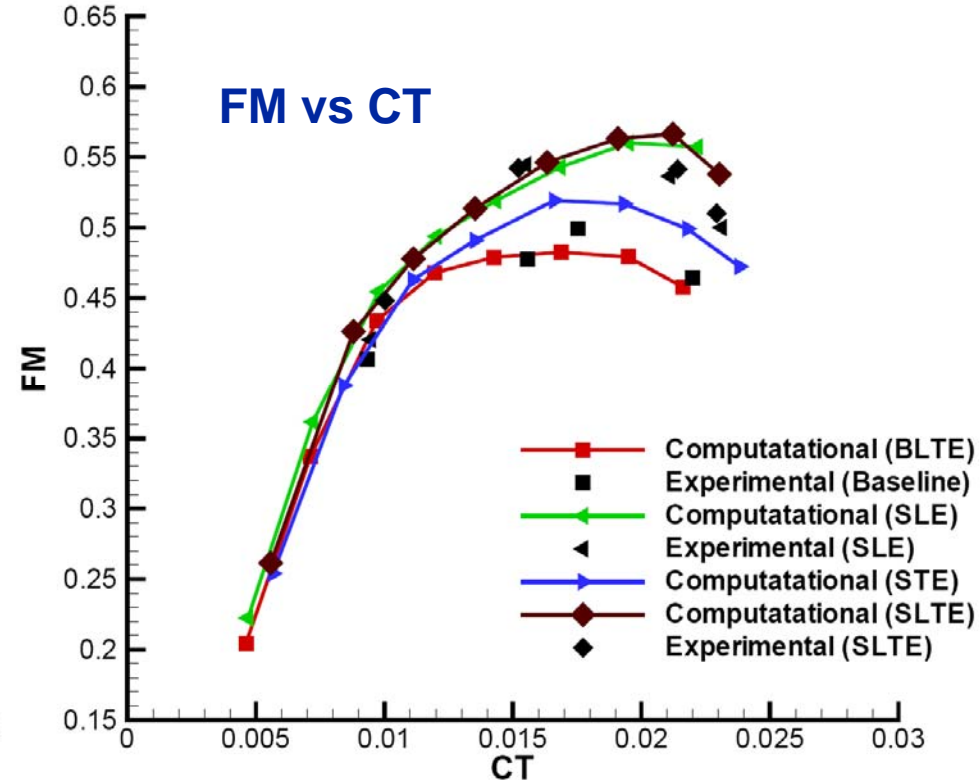
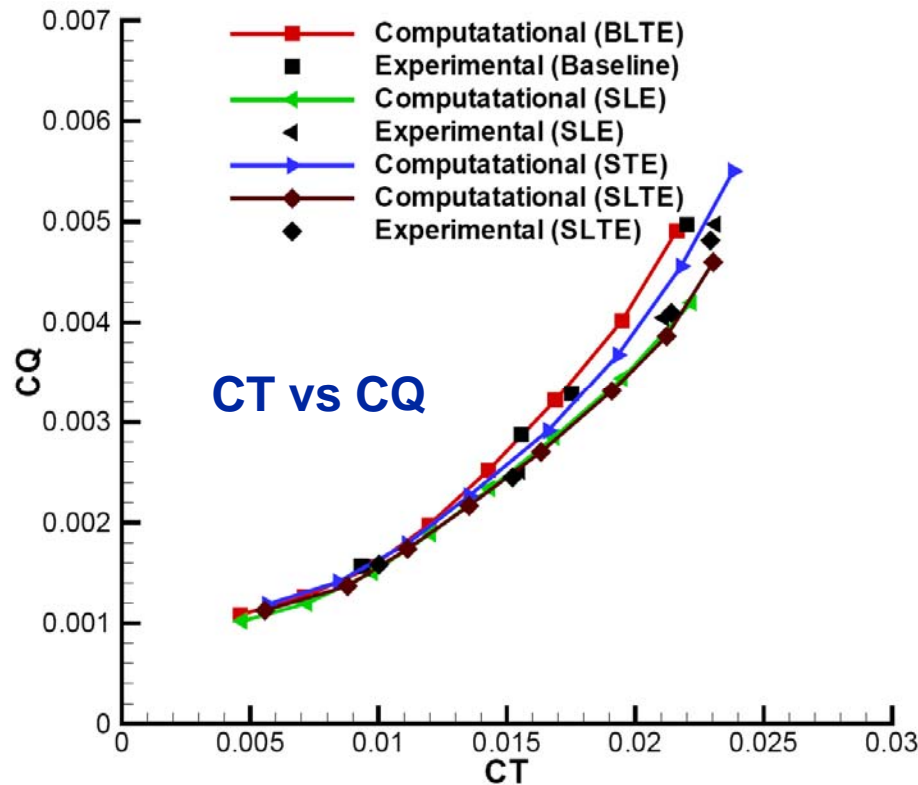
Performance Comparison



Reasonably good comparison between CFD and experiment



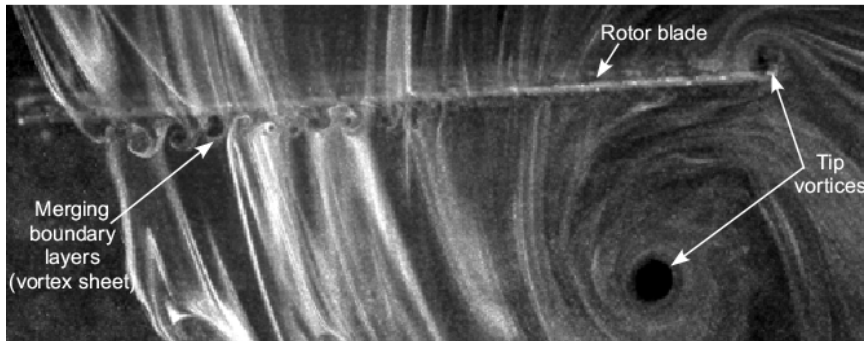
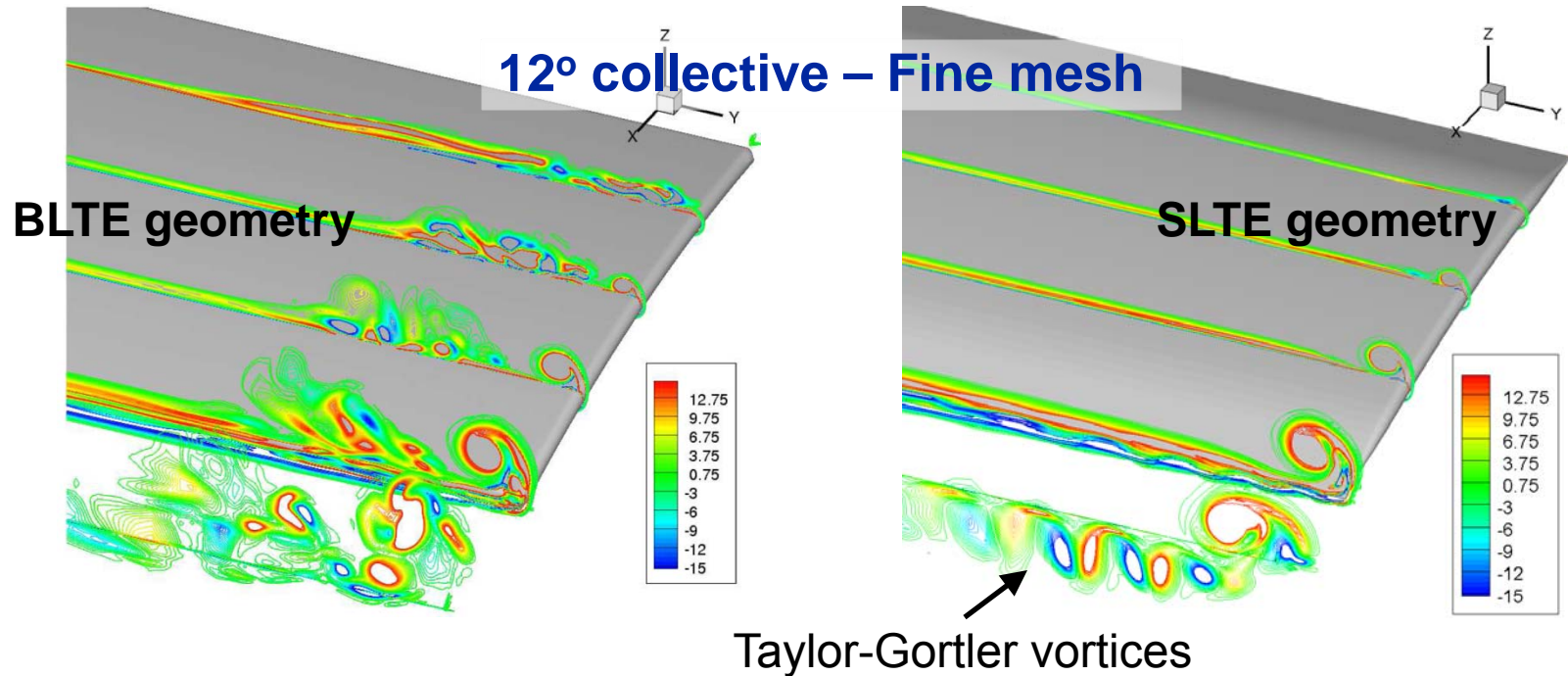
Performance Comparison



Reasonably good comparison between CFD and experiment



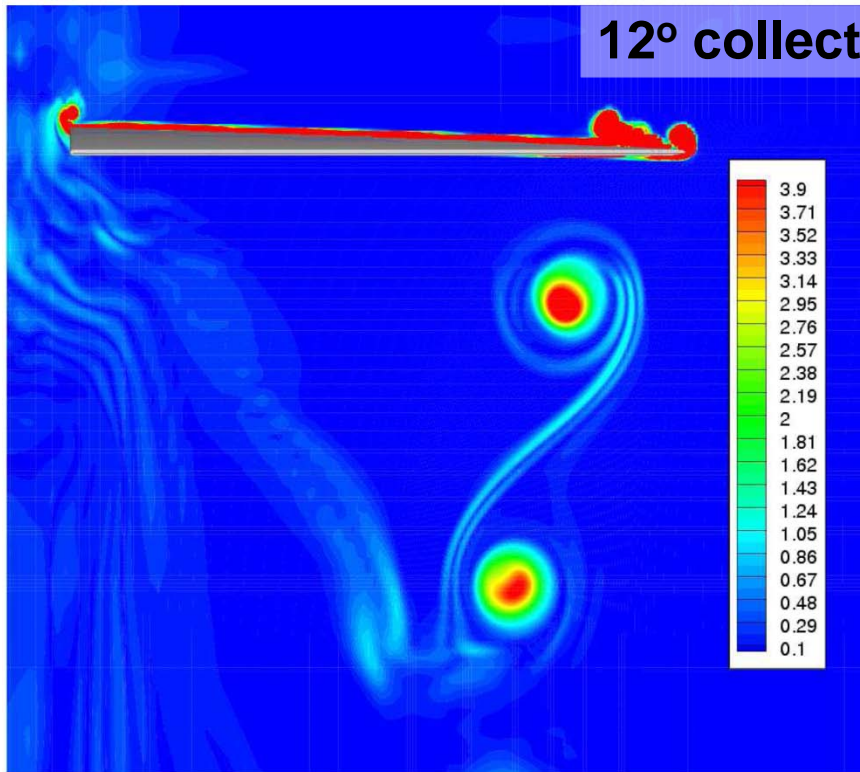
Streamwise Vorticity Contour



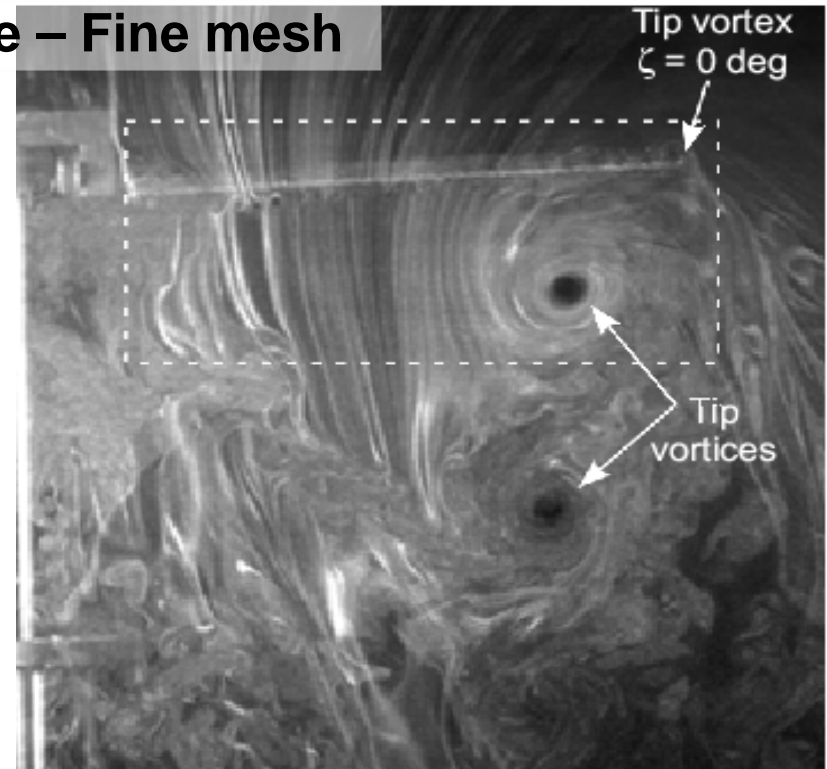
Experimental Flow Visualization.
Courtesy: Ramasamy, Leishman and Lee



Flow-Field Visualization (BLTE geometry)



Vorticity magnitude contours, $\psi=0^\circ$.
(Blunt leading edge geometry)



Experimental Flow Visualization.
Courtesy :Ramasamy, Leishman and Lee

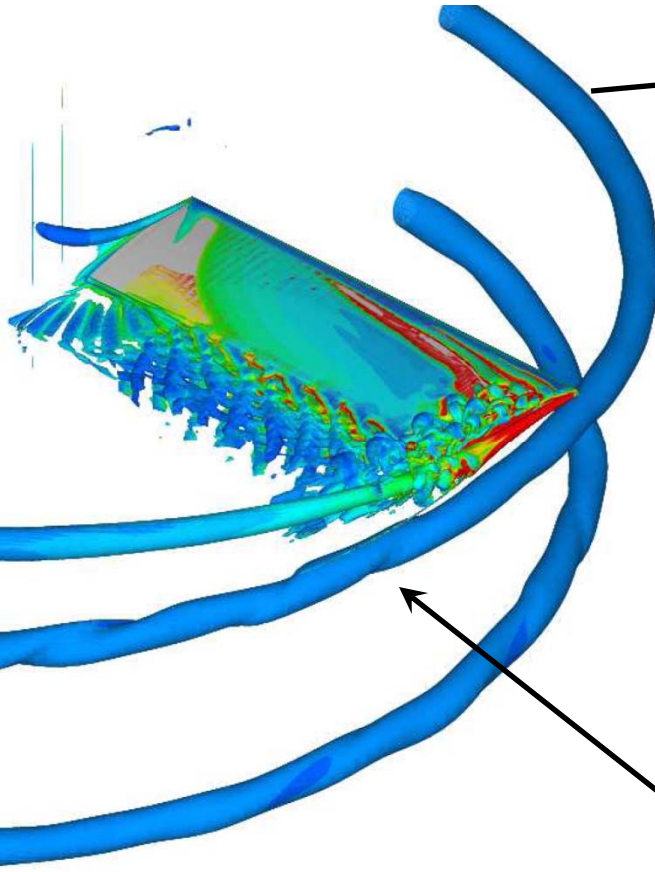
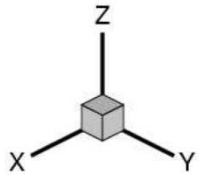
- **Wake Structures are very similar**



Flow-Field Visualization (BLTE geometry)



12° collective – Fine mesh



From second blade

Iso-surfaces of q-criterion, $q = 1.0$.

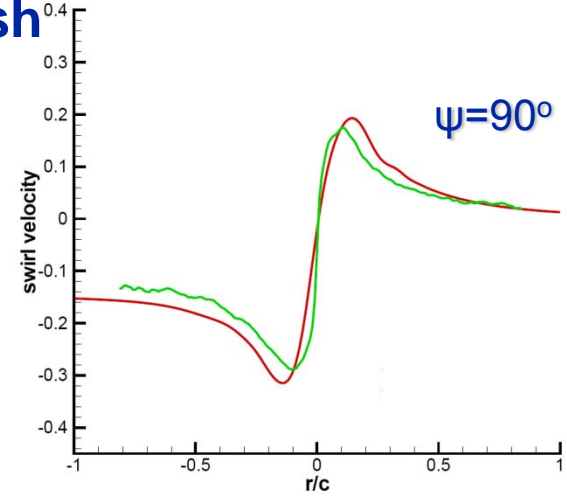
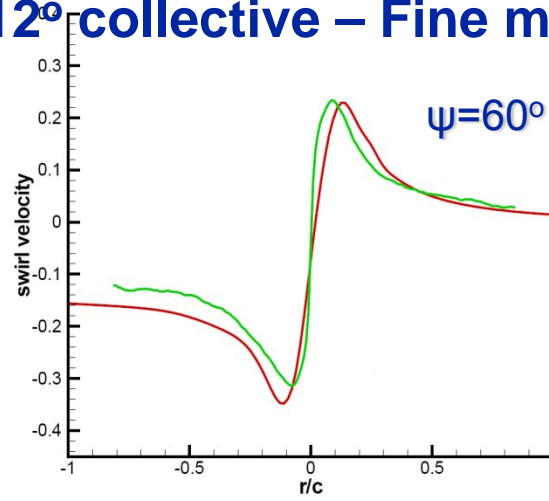
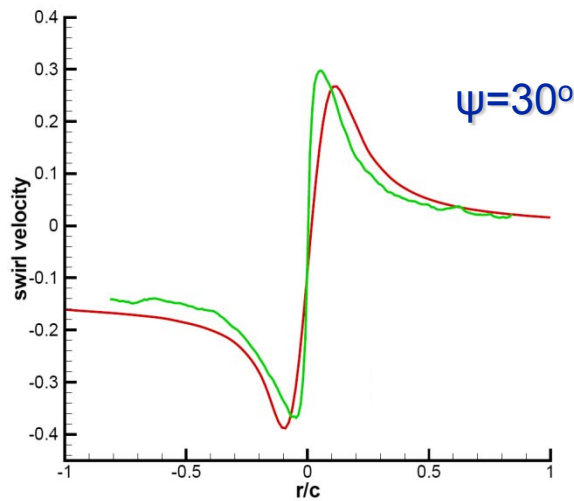
Twisting of vortices
after blade passage



Vortex Structure – Swirl Velocity (BLTE geometry)

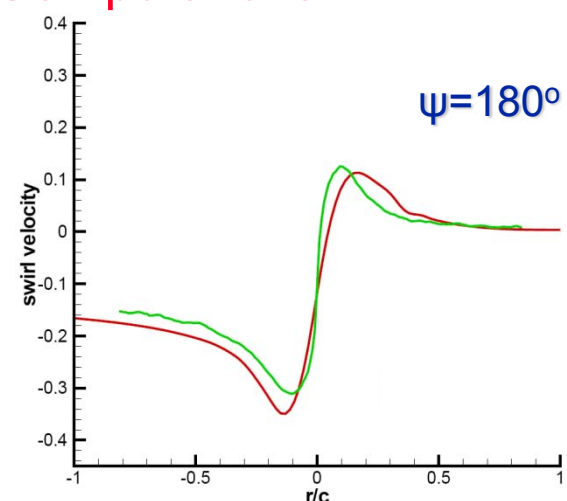
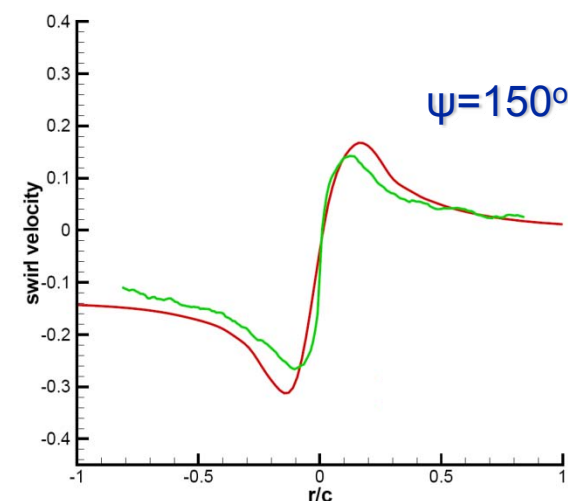
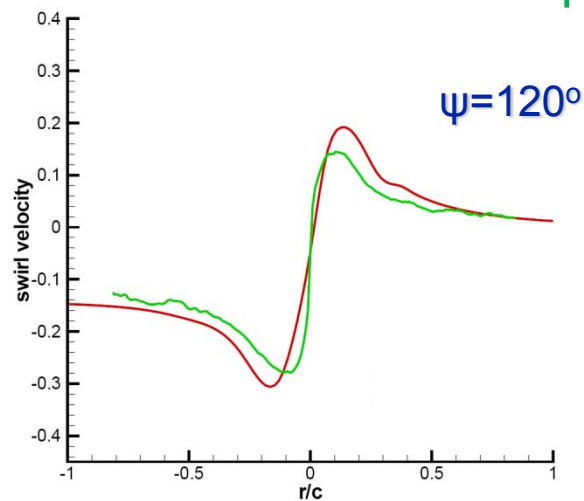


12° collective – Fine mesh



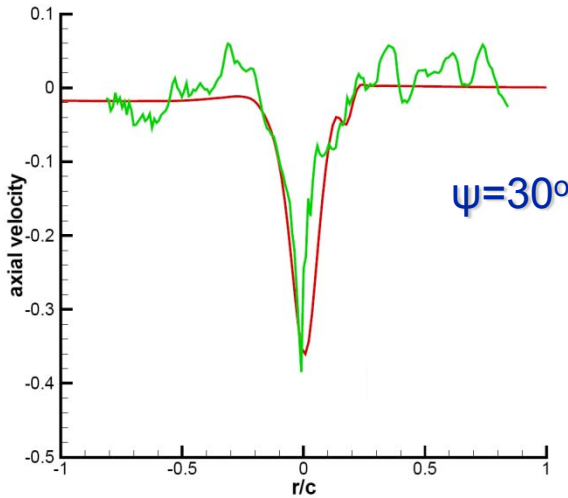
— Experimental

— Computational

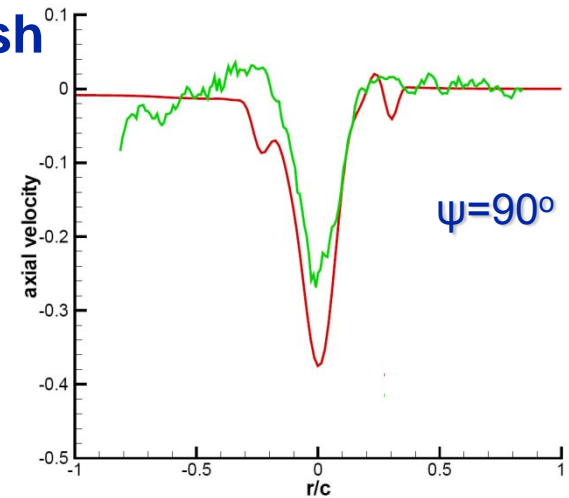
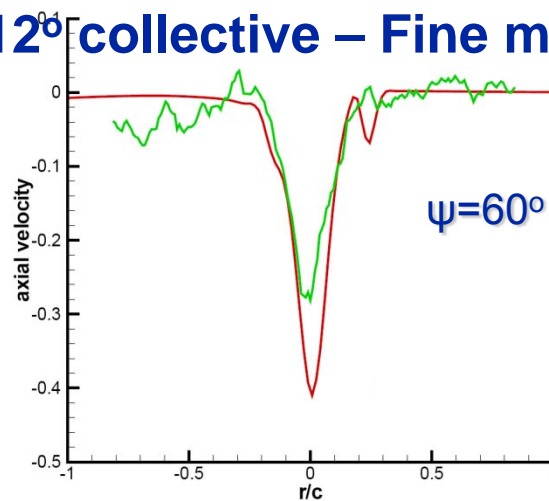




Vortex Structure – Axial Velocity (BLTE geometry)

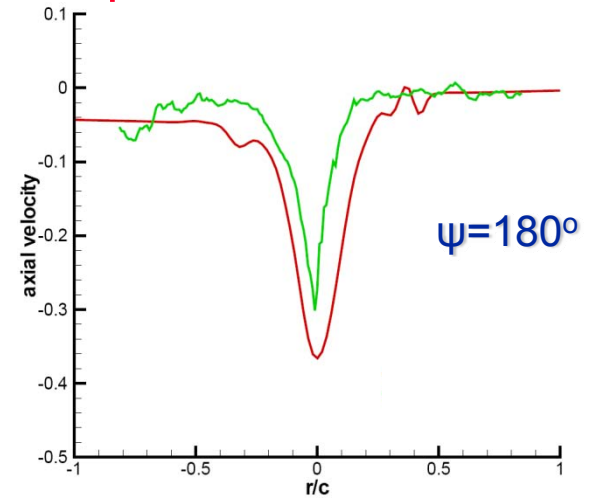
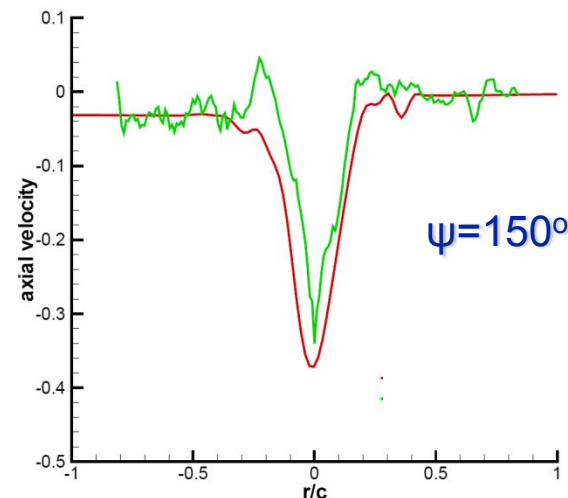
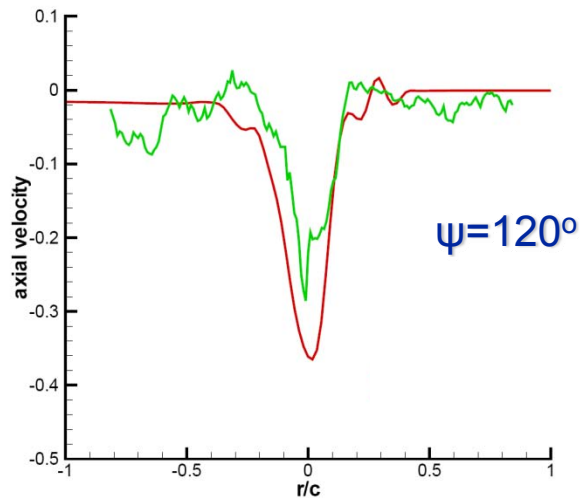


12° collective – Fine mesh



— Experimental

— Computational





Micro-Scale Single Rotor in Ground Effect



Experimental Setup for Validation



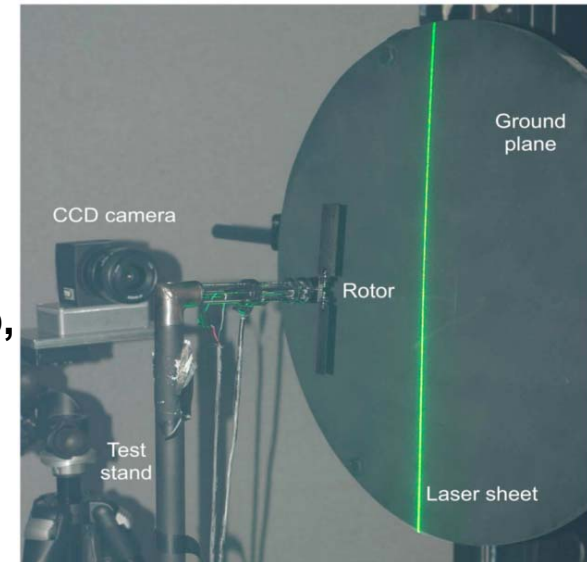
- **2-bladed rotor setup of Lee et al.**

- BLTE rotor of Ramasamy et al.
- Collective setting of 12°

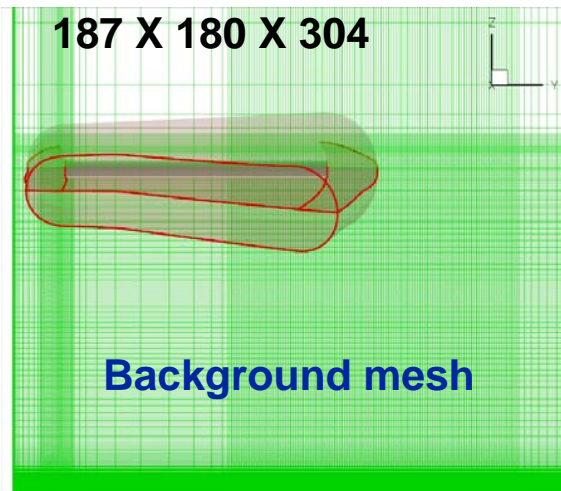
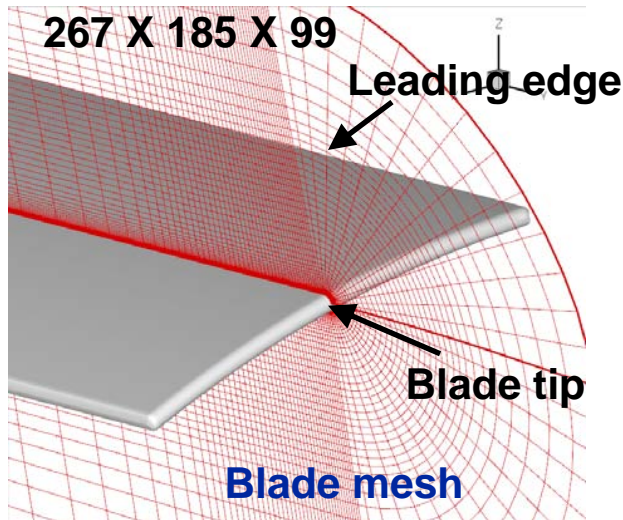
- **Ground plane distances**

- $h/R = 0.25$ to 4.0

Experimental Setup,
Lee et al.



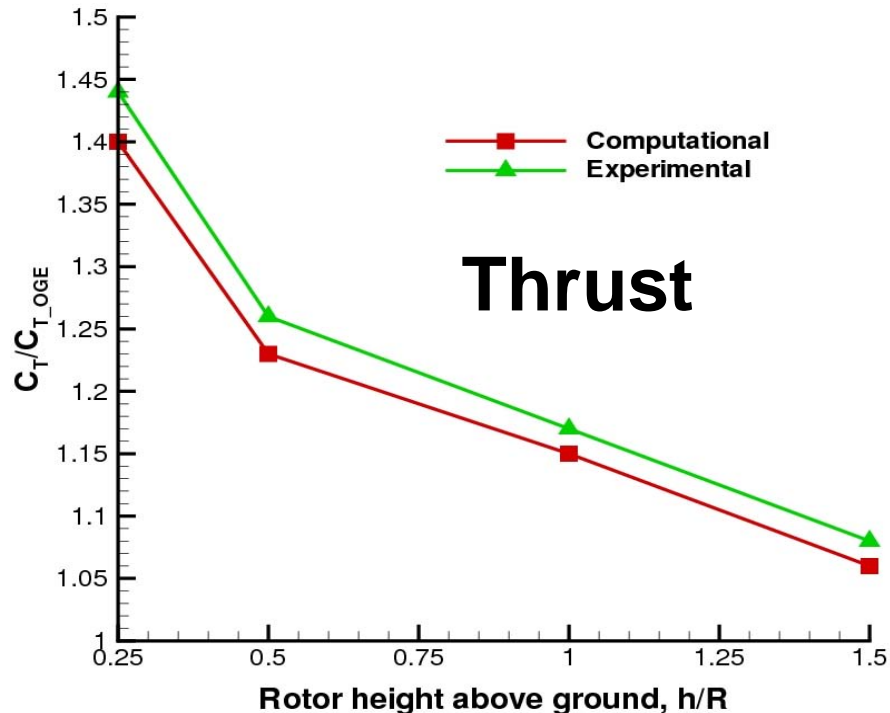
Mesh System



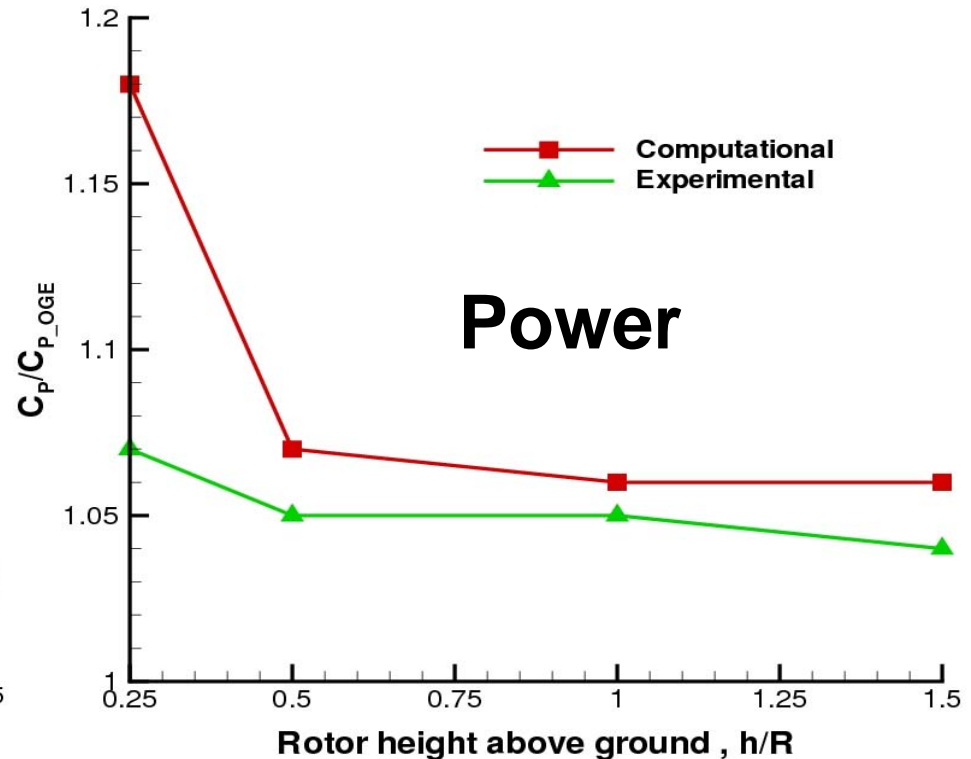
9.8 million mesh points



Performance Comparison



$C_{T(OGE), \text{computational}} = 0.0143$
 $C_{T(OGE), \text{experimental}} = 0.0133$

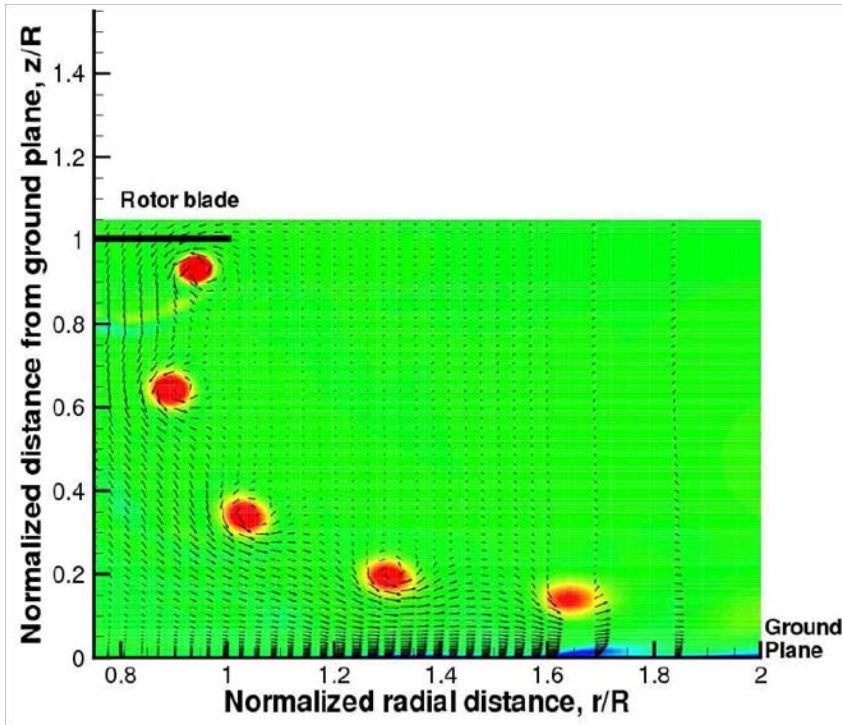


$C_{P(OGE), \text{computational}} = 0.00277$
 $C_{P(OGE), \text{experimental}} = 0.00249$

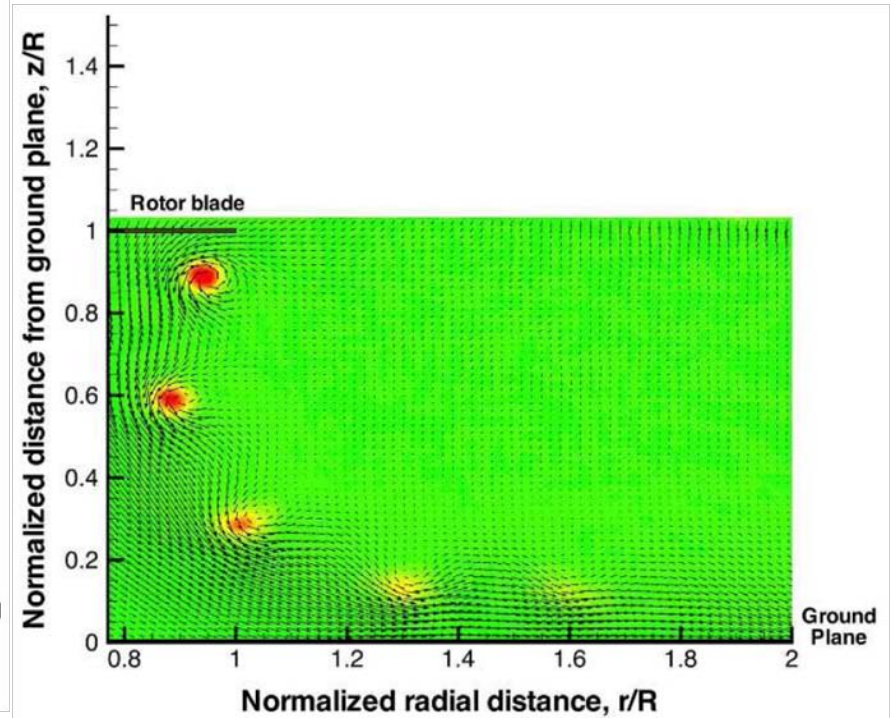
- Good agreement, except for power at $h/R = 0.25$



Vortex Trajectory Comparison, $h/R = 1.0$



Computational, $\Psi = 60^\circ$

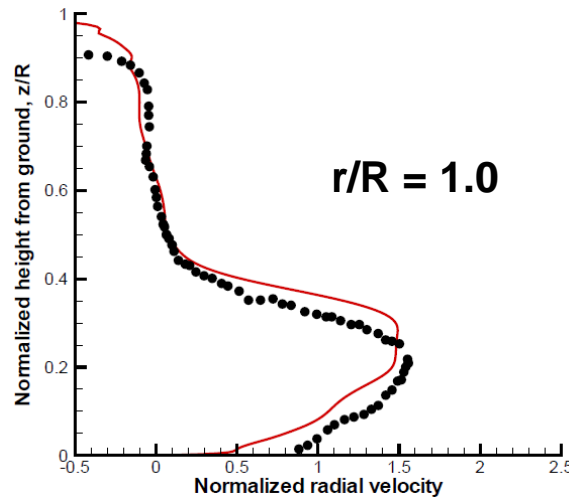
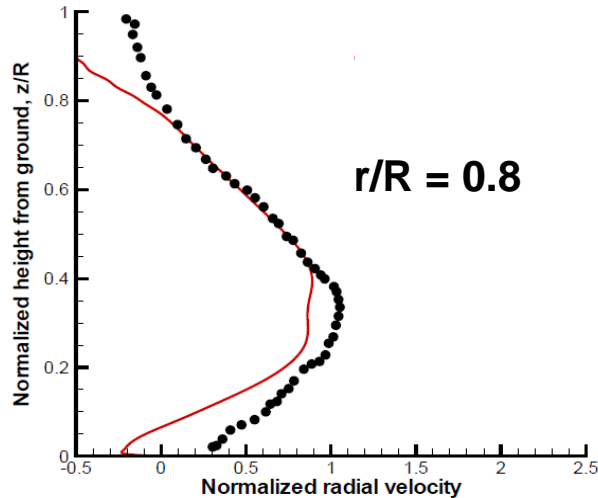


Experimental, $\Psi = 60^\circ$

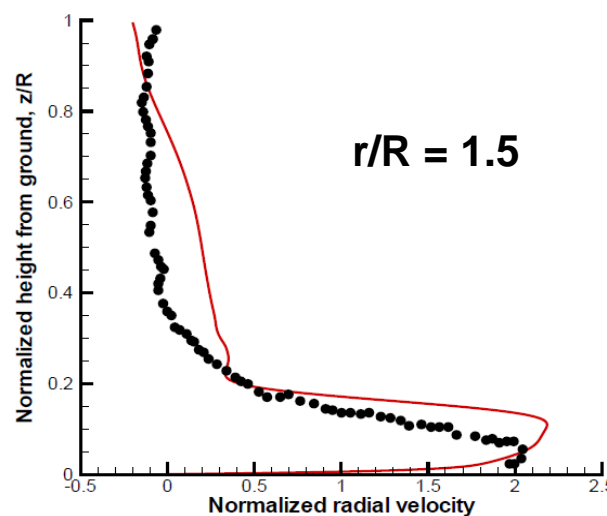
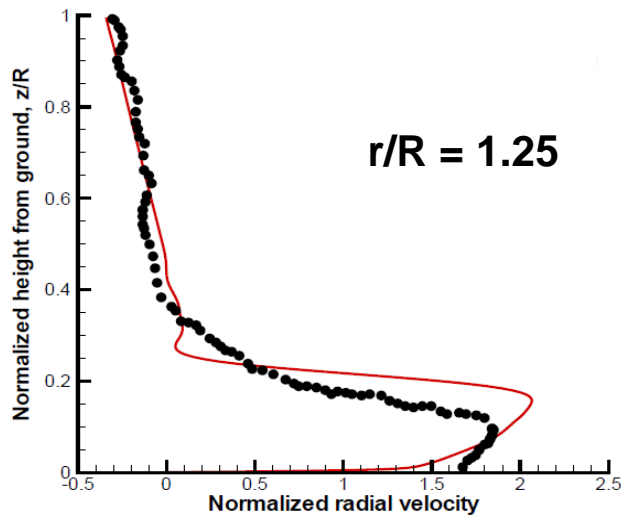
- Good agreement of vortex positions
- Increased wandering in experiment increases effective core size



Time-Averaged Radial Velocity, $h/R = 1.0$



— Computational
• Experimental



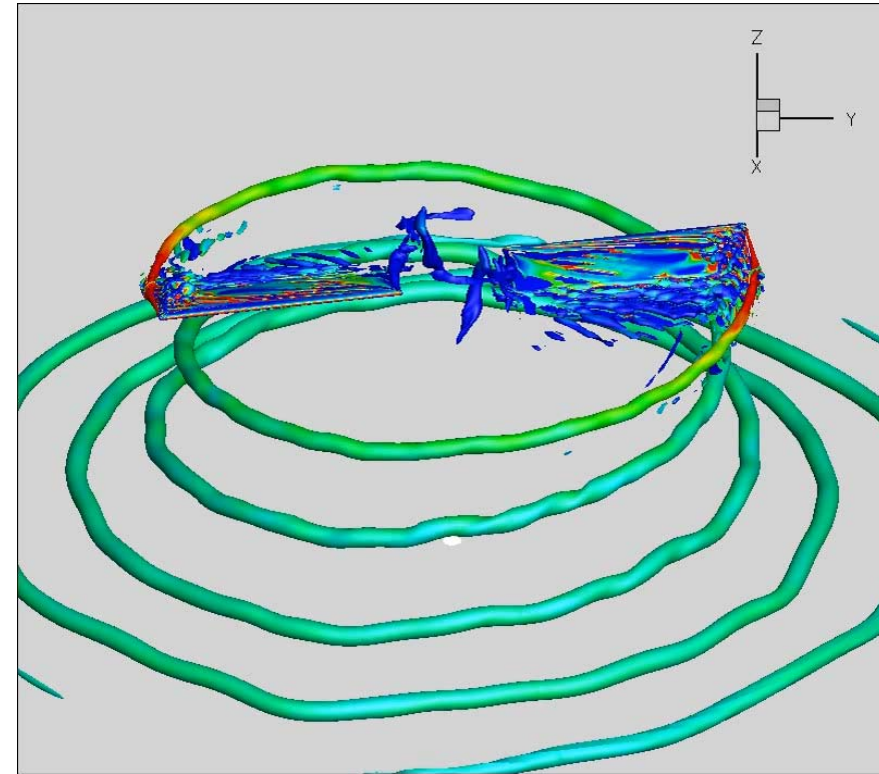
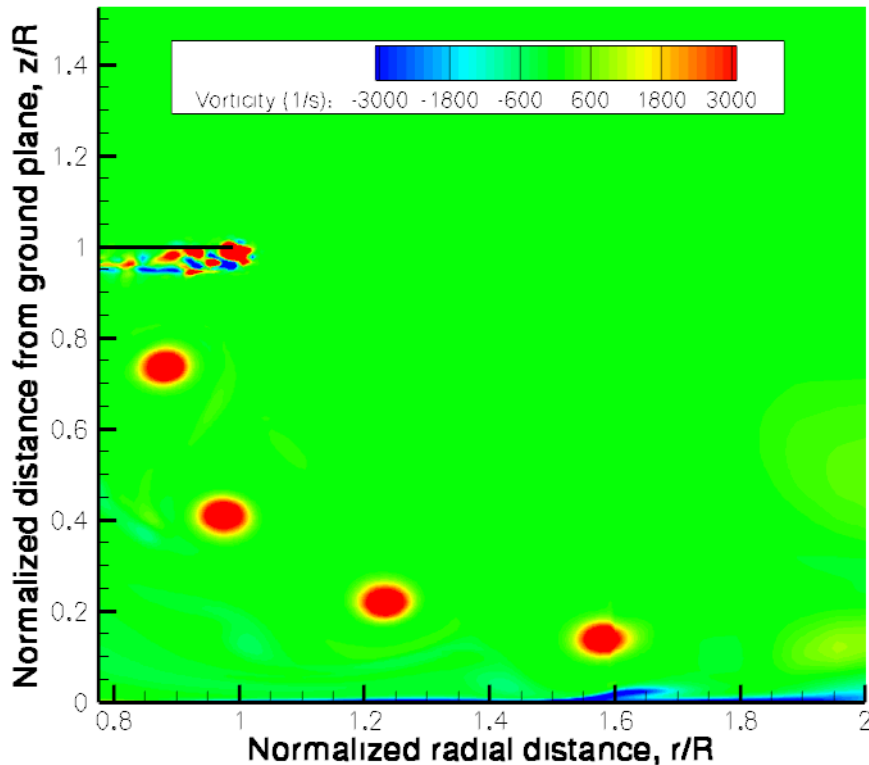
Good comparison,
especially at inboard
locations



Flow Visualization, $h/R = 1.0$



Vorticity Contour



Iso-surface of q -criterion, $q = 4.0$

- Tip vortex resolved for over 2+ rotor revolutions
- Development of instabilities



Micro-Scale Coaxial Rotor



Experimental Setup (Micro-Scale Coaxial Rotor)



Two 2-bladed rotor setup of Bohorquez and Pines

- Untwisted rectangular
- Aspect Ratio of 4.98
- Collective setting of 16°

Airfoil profile

- Circular Arc with sharp leading and trailing edge
- 2.2% Thickness
- 6% Camber

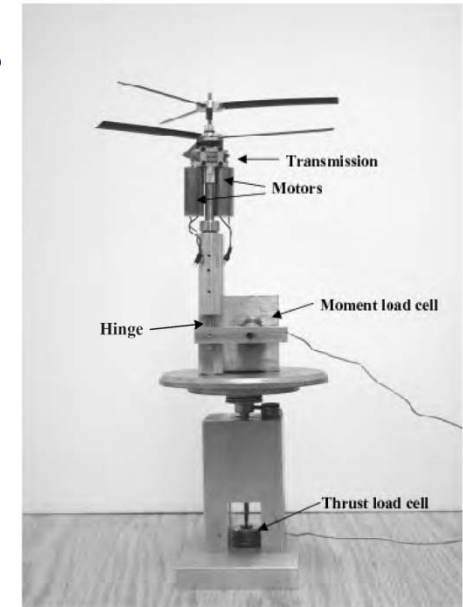
Flow conditions

- RPM → 1900 to 2700
- Re_{tip} → 19,000 to 27,000
- M_{tip} → 0.0665 to 0.0945

Torque balanced by adjusting bottom rotor RPM

- Percentile difference less than 2%

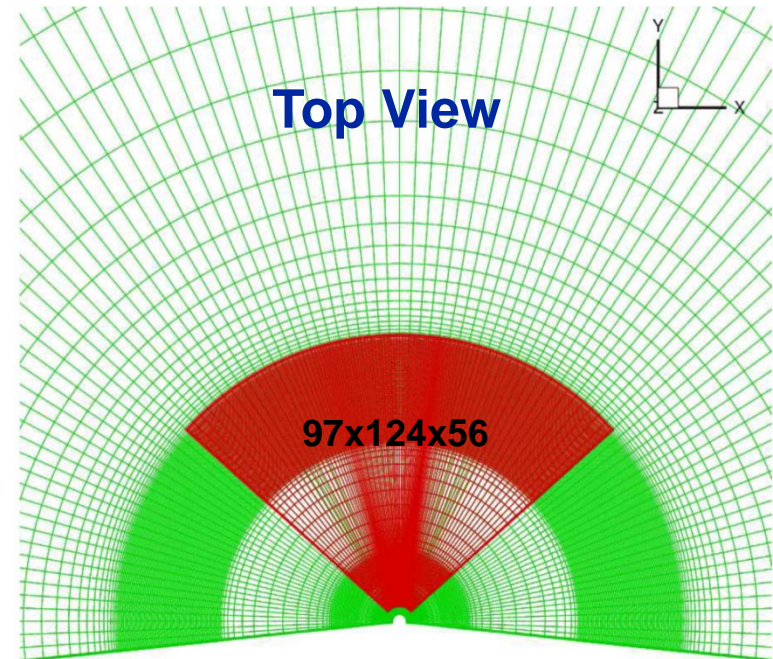
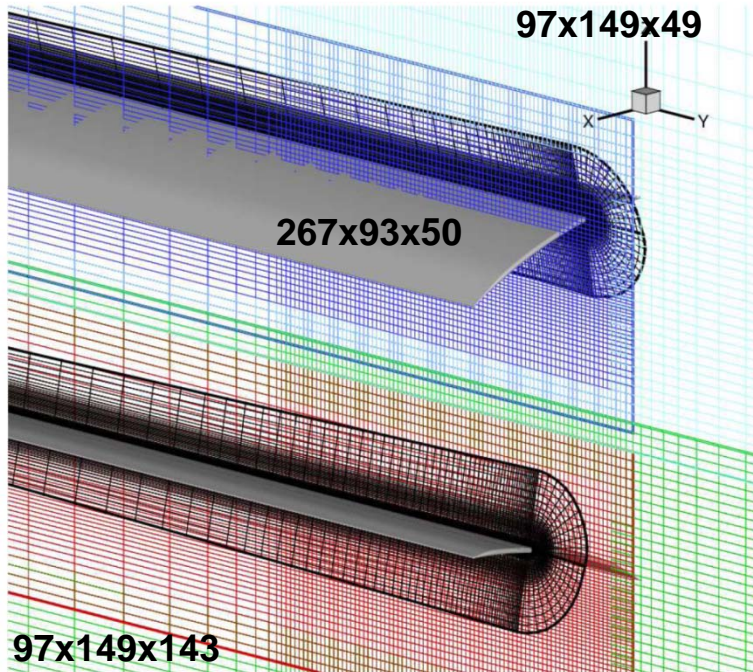
Computations performed assuming identical RPM



Experimental setup
Bohorquez and Pines (Univ of Maryland)



Mesh System



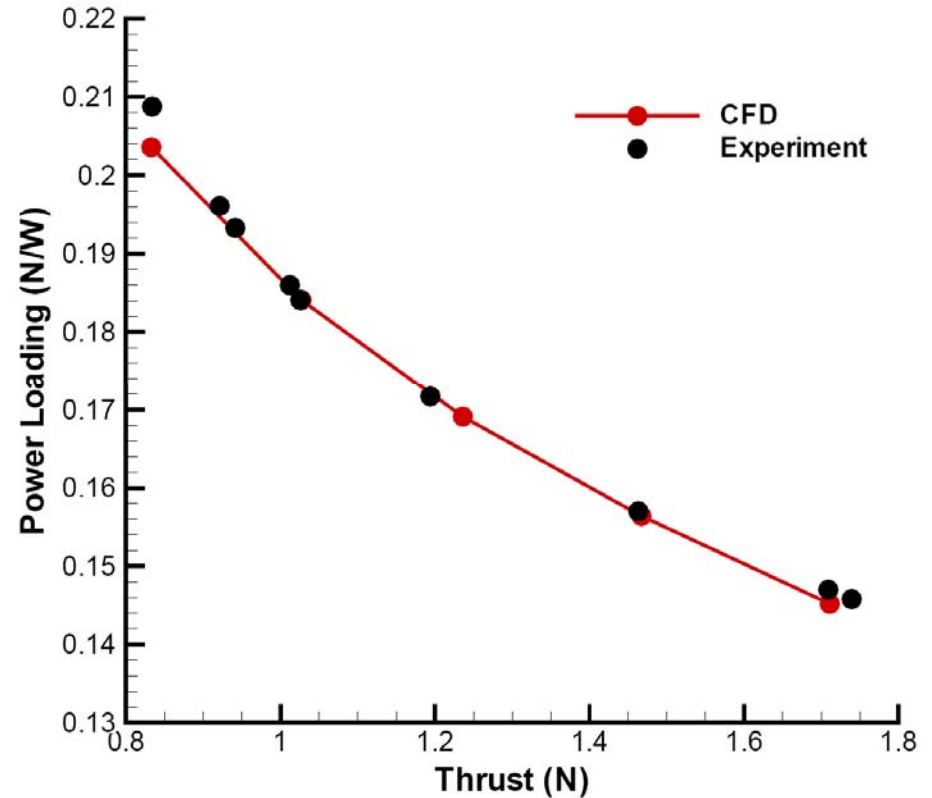
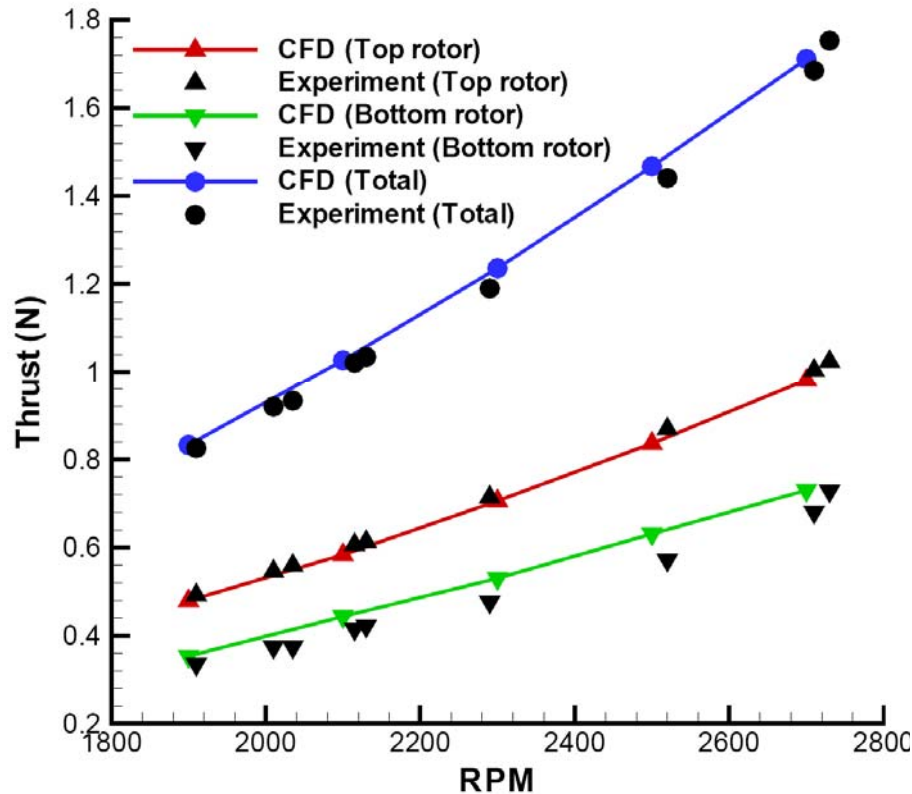
- **Total mesh points ~ 6.6 million**
- **In most refined regions**

➔ $\Delta r = 0.025$ chords, $\Delta z = 0.02$ chords, $\Delta\psi = 0.3^\circ$, inner background

➔ $\Delta r = 0.025$ chords, $\Delta z = 0.04$ chords, $\Delta\psi = 2^\circ$, outer background



Effect of RPM ($h/R = 0.446$)



Performance well predicted



Effect of Rotor Spacing (Mean Thrust)



h/R	C_T (top rotor)	C_T (bottom rotor)	C_T (total)	$C_{T_{top}}/C_{T_{total}}$	$C_{T_{total}}$ (Expt.)
0.268	0.0199	0.0163	0.0362	0.55	0.0349
0.357	0.0205	0.0158	0.0363	0.56	0.0349
0.446	0.0208	0.0157	0.0365	0.57	0.0350
0.536	0.0210	0.0155	0.0365	0.58	0.0350
0.625	0.0212	0.0153	0.0365	0.58	0.0350

- **As rotor spacing increases**
 - ➔ Induced inflow on top rotor decreases
 - ➔ Inflow on bottom rotor increases



Effect of Rotor Spacing (Unsteady Thrust)



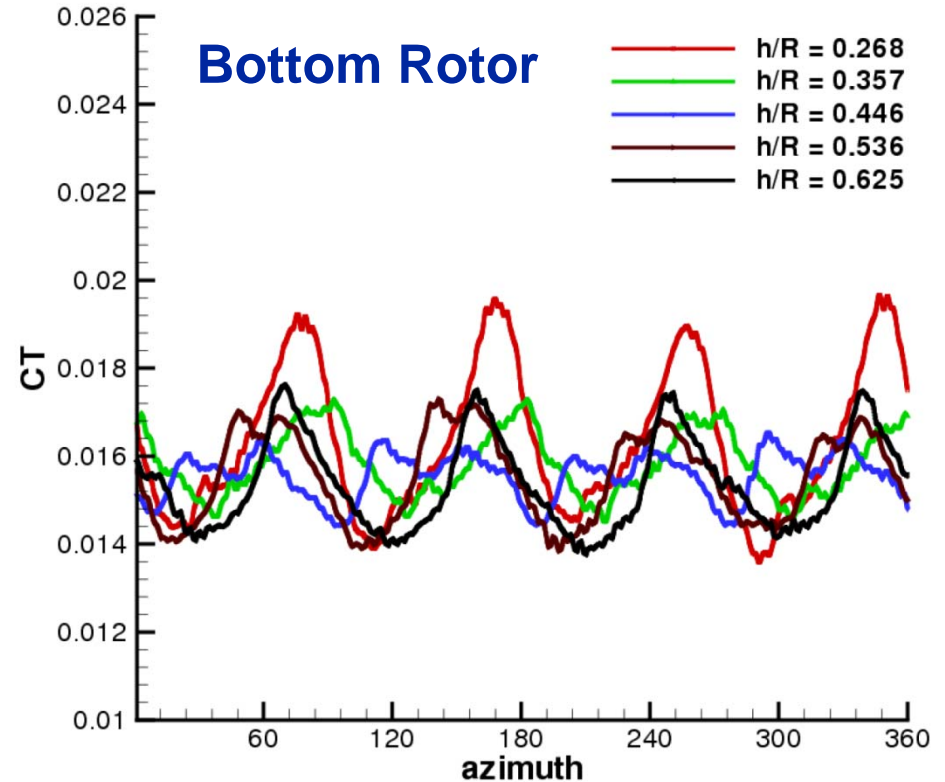
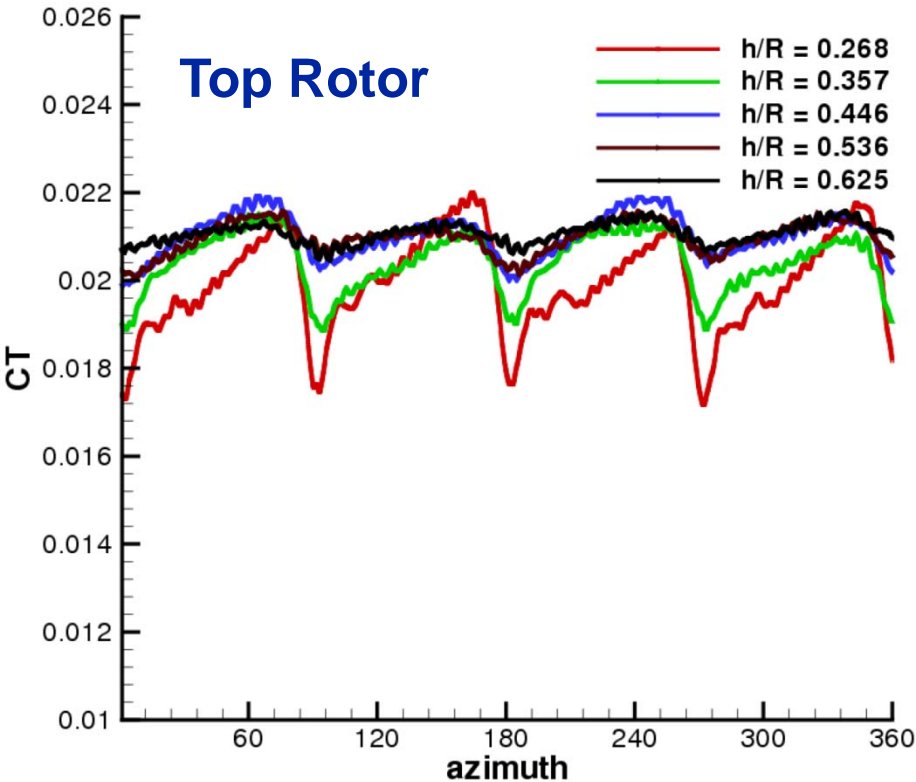
h/R	% fluctuation (top rotor)	% fluctuation (bottom rotor)	% fluctuation (total)
0.268	5.28%	10.06%	6.55%
0.357	3.17%	4.68%	2.04%
0.446	1.92%	3.63%	2.41%
0.536	1.71%	5.87%	3.29%
0.625	1.13%	6.86%	3.21%

- **As rotor spacing increases**
 - Unsteadiness in top rotor → decreases
 - Unsteadiness in bottom rotor → No trend (Different from full-scale)
- **3 – 8% fluctuation**
 - Significant for vibration and acoustic characteristics

Challenging to capture unsteadiness in experiments



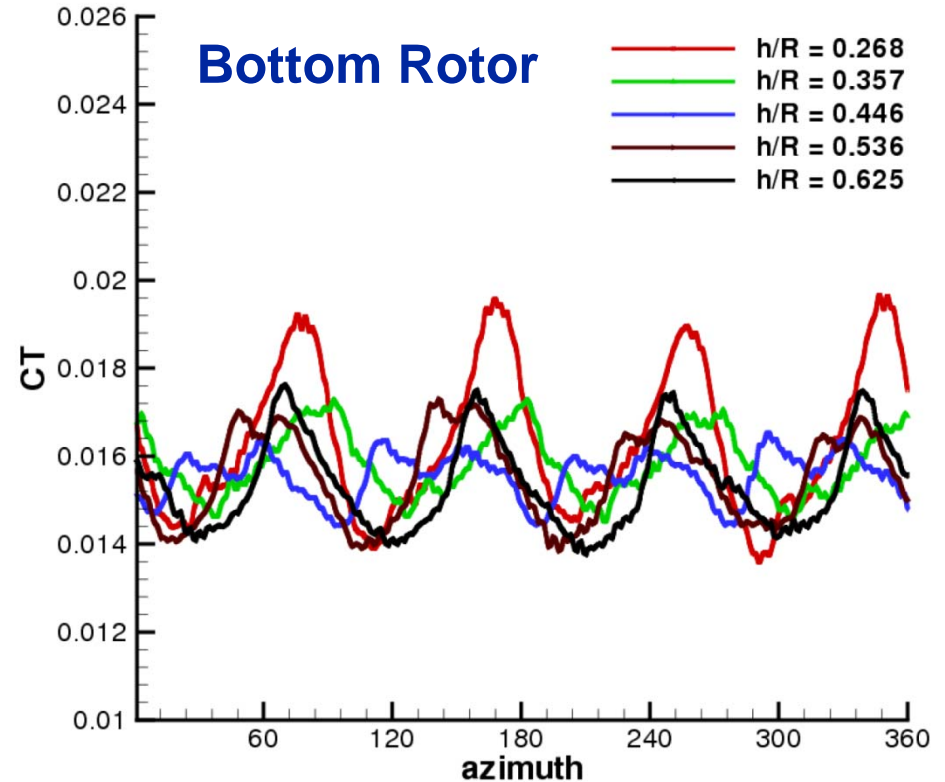
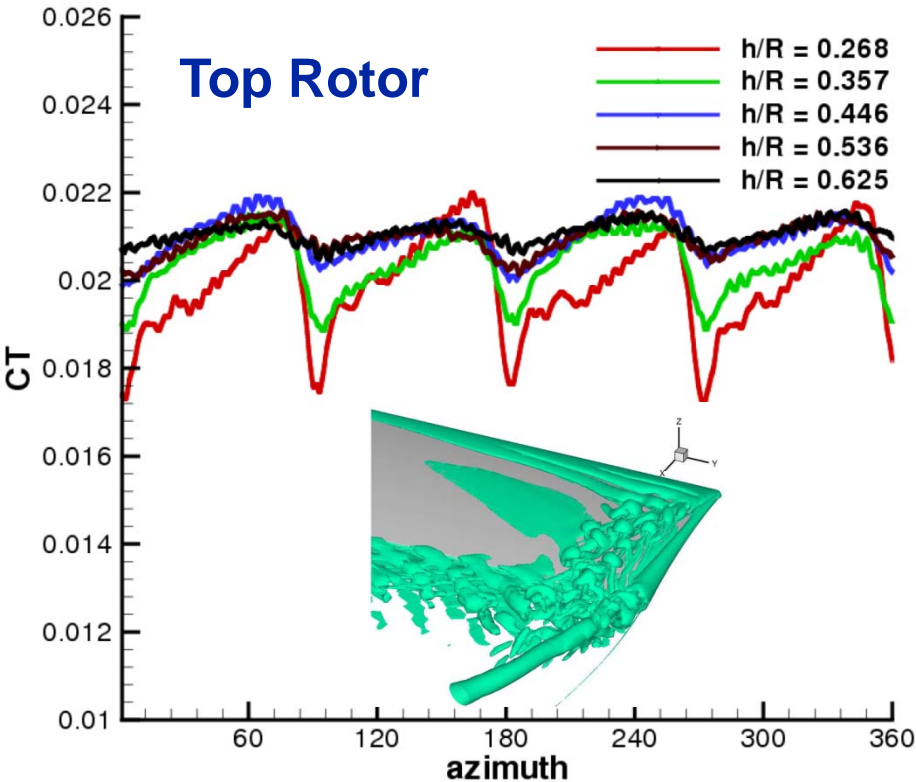
Temporal Variation of Thrust



- **Dominant 4/rev frequency**
- **Unsteadiness caused by**
 - Loading effect
 - Wake effect
 - Shedding near trailing edge → High frequency unsteadiness



Temporal Variation of Thrust

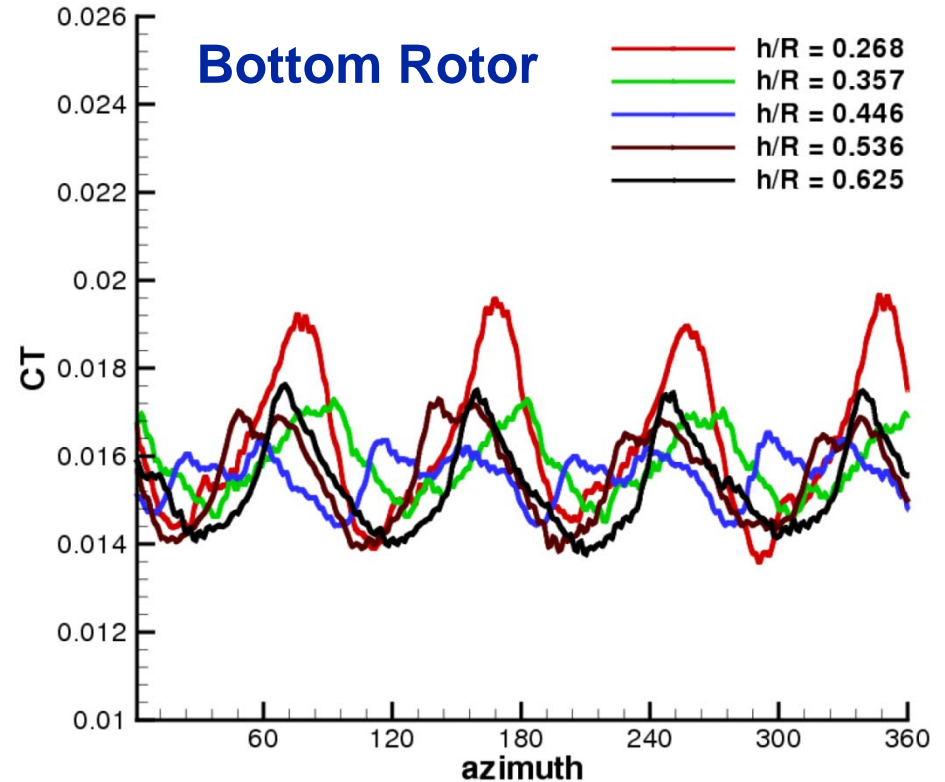
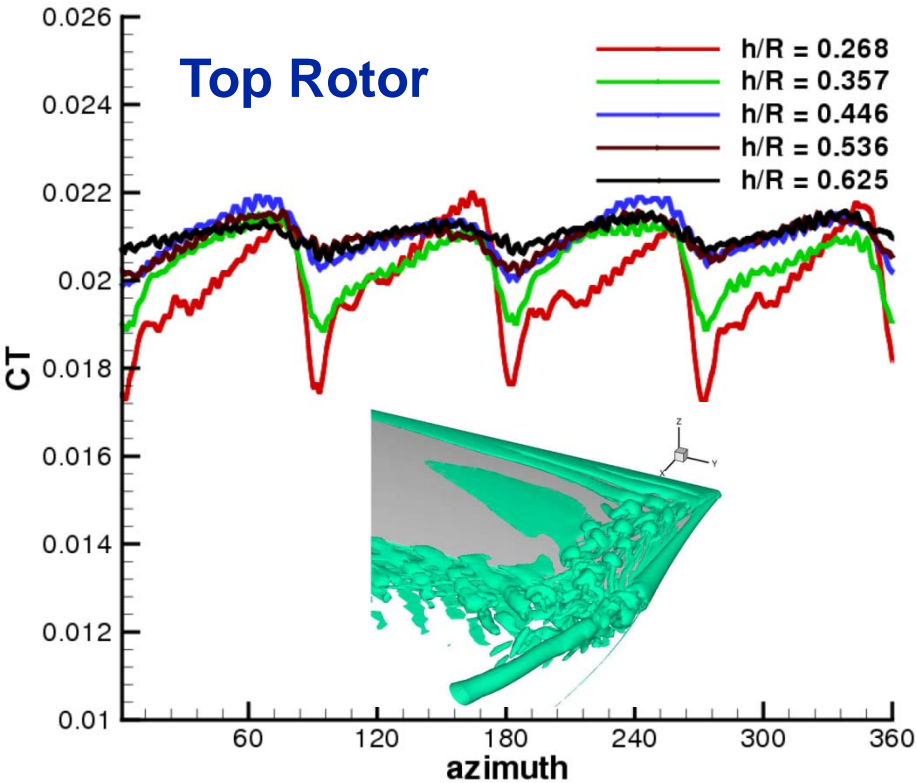


- Dominant 4/rev frequency
- Unsteadiness caused by

- Loading effect
- Wake effect
- Shedding near trailing edge → High frequency unsteadiness



Temporal Variation of Thrust



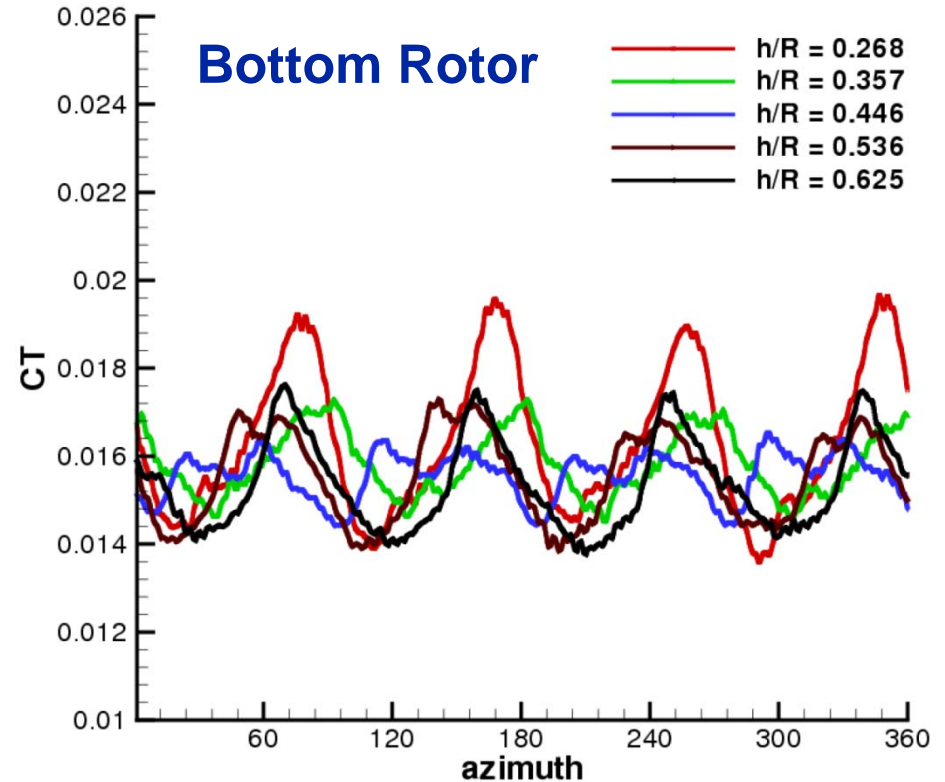
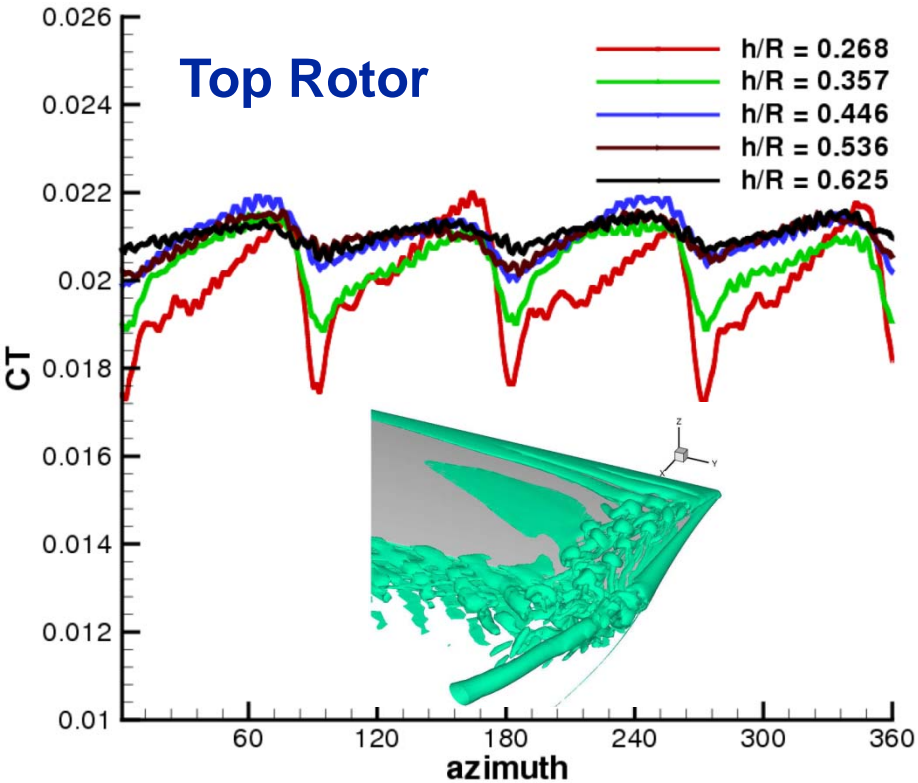
- **As rotor spacing increases**

- ➔ Unsteadiness in top rotor → decreases

- ➔ Unsteadiness in bottom rotor → No trend (Different from full-scale)



Temporal Variation of Thrust

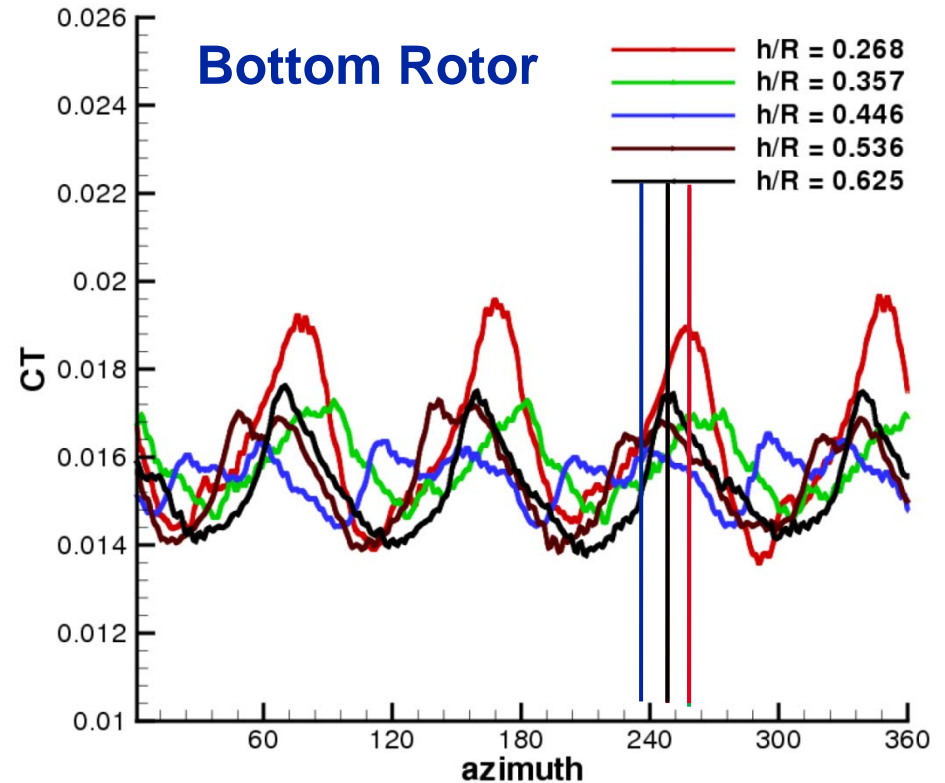
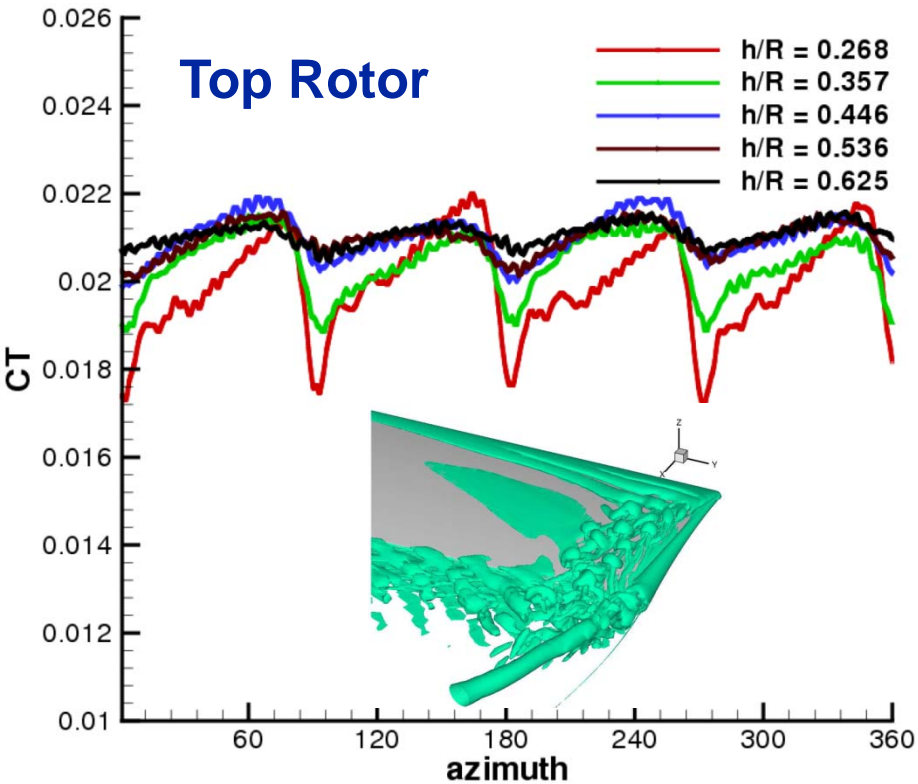


- **Two Peaks**

- ➔ Loading effect
- ➔ Vortex impingement



Temporal Variation of Thrust

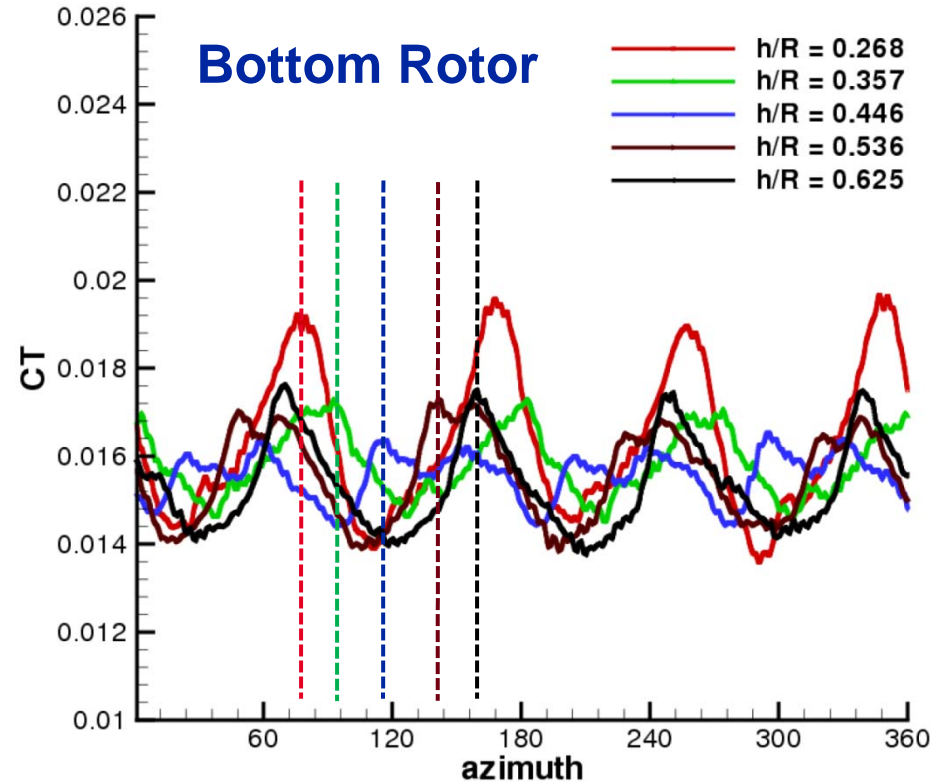
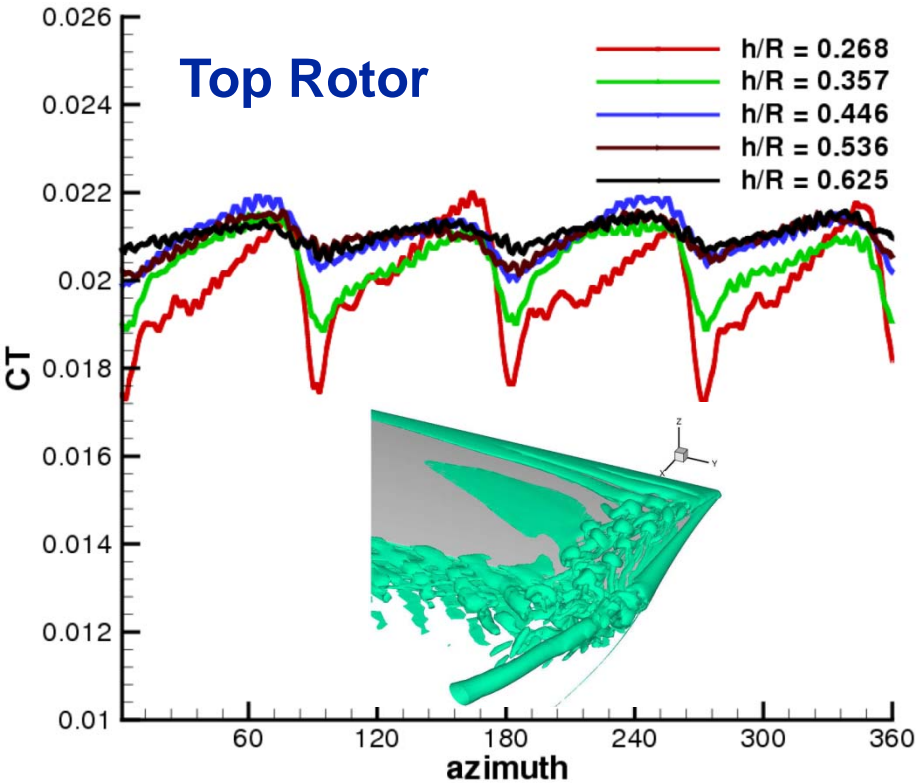


- **Two Peaks**

- ➔ Loading effect
- ➔ Vortex impingement



Temporal Variation of Thrust

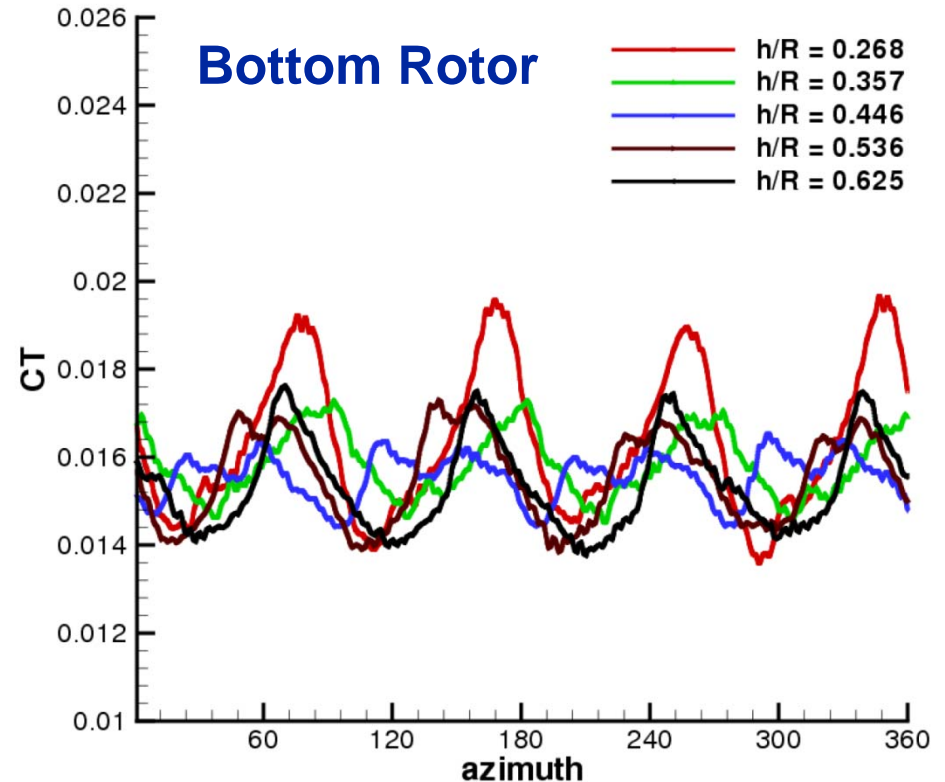
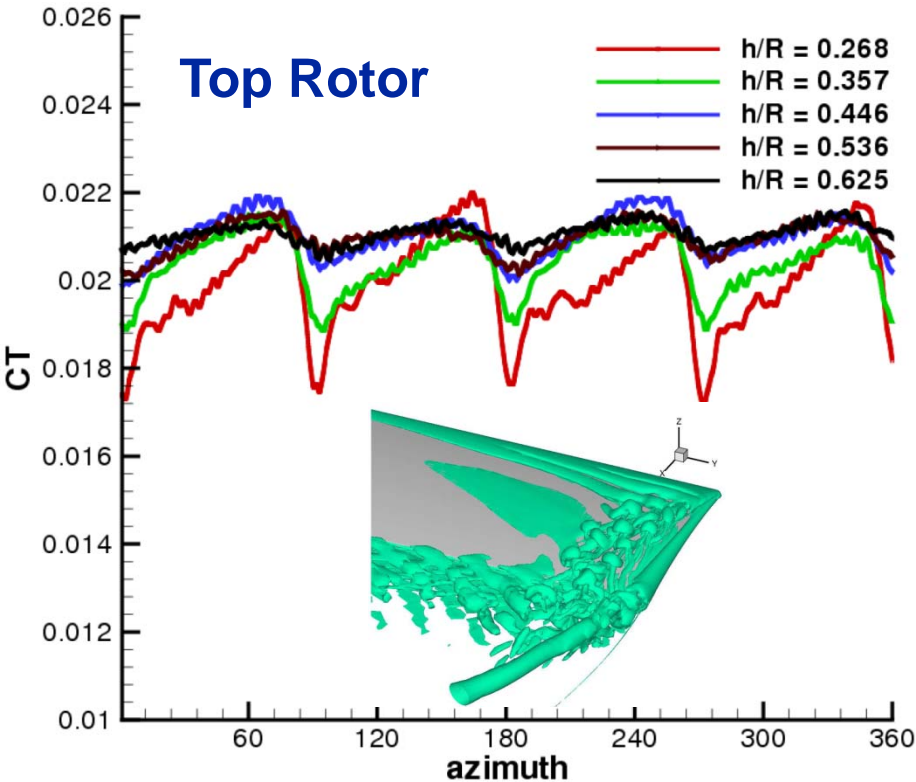


- **Two Peaks**

- ➔ Loading effect
- ➔ Vortex impingement



Temporal Variation of Thrust

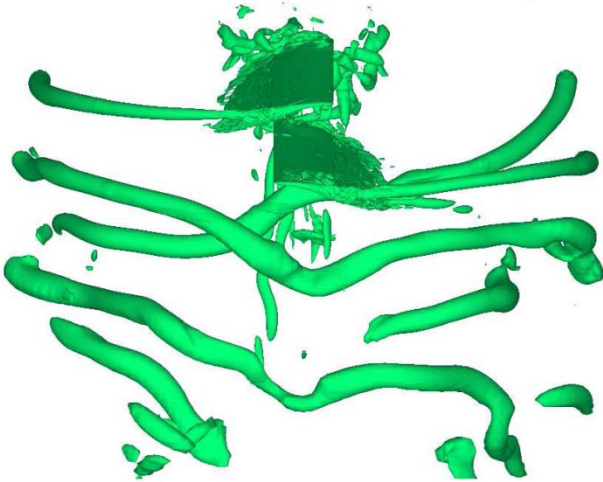
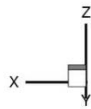


- **Phasing of vortex impingement is significant**

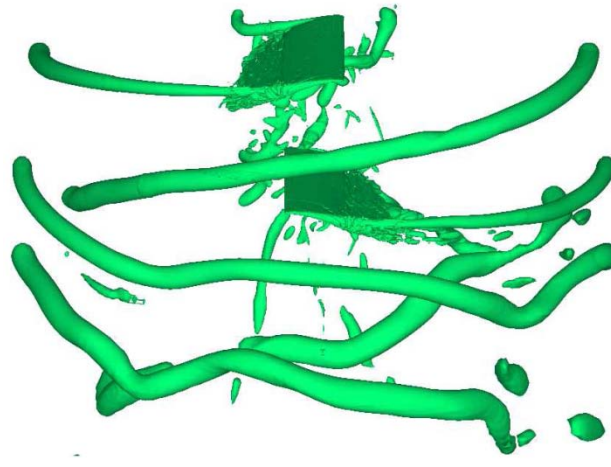
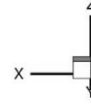
- ➔ When peaks coincide, large unsteadiness
- ➔ When peaks are farthest apart, smaller unsteadiness



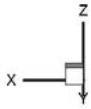
Wake Trajectory



$h/R = 0.268$



$h/R = 0.446$



$h/R = 0.625$

Iso-surface of q -criterion, $q = 0.2$

- Tip vortex resolved for 2-blade passage
- Significant interaction between top and bottom rotor wake
- Straining in the top rotor vortices as it passes bottom rotor





Micro-Scale Shrouded Rotor



Micro-Scale Shrouded Rotor



Setup of Hrishikeshavan and Chopra

Rotor Configuration

- 2 bladed with 2:1 taper from 60%R
- Aspect Ratio of 4.84
 - 121mm radius and 25mm chord

Airfoil profile

- Circular arc w/ LE sharpened from 8% chord
- 2% Thickness & 10% Camber

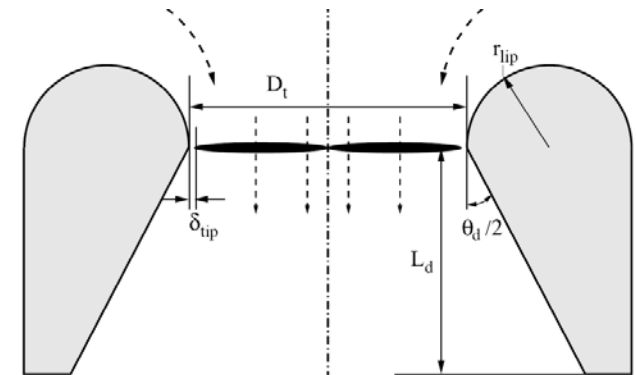
Shroud Configuration

- Throat diameter (D_t)
- Tip clearance (δ_{tip})
- Lip radius (r_{lip})
- Diffuser length (L_d)
- Diffuser angle (θ_d)
- Shape of outer portion of shroud not significant



Experimental setup

- Hrishikeshavan and Chopra



Schematic of shroud



Micro-Scale Shrouded Rotor



Setup of Hrishikeshavan and Chopra

Rotor Configuration

- 2 bladed with 2:1 taper from 60%R
- Aspect Ratio of 4.84
 - 121mm radius and 25mm chord

Airfoil profile

- Circular arc w/ LE sharpened from 8% chord
- 2% Thickness & 10% Camber

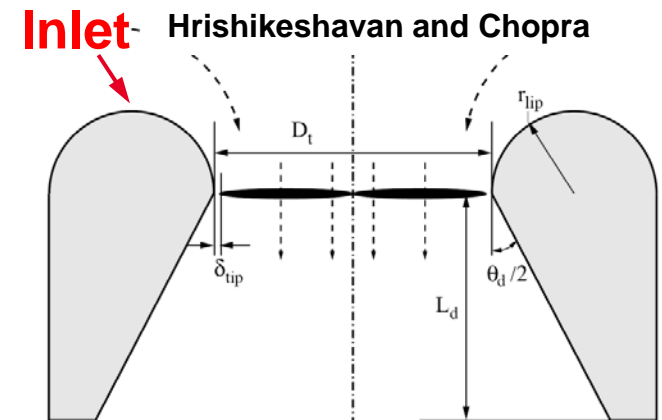
Shroud Configuration

- Throat diameter (D_t)
- Tip clearance (δ_{tip})
- Lip radius (r_{lip})
- Diffuser length (L_d)
- Diffuser angle (θ_d)
- Shape of outer portion of shroud not significant



Experimental setup

Hrishikeshavan and Chopra



Schematic of shroud



Micro-Scale Shrouded Rotor



Setup of Hrishikeshavan and Chopra

Rotor Configuration

- 2 bladed with 2:1 taper from 60%R
- Aspect Ratio of 4.84
 - 121mm radius and 25mm chord

Airfoil profile

- Circular arc w/ LE sharpened from 8% chord
- 2% Thickness & 10% Camber

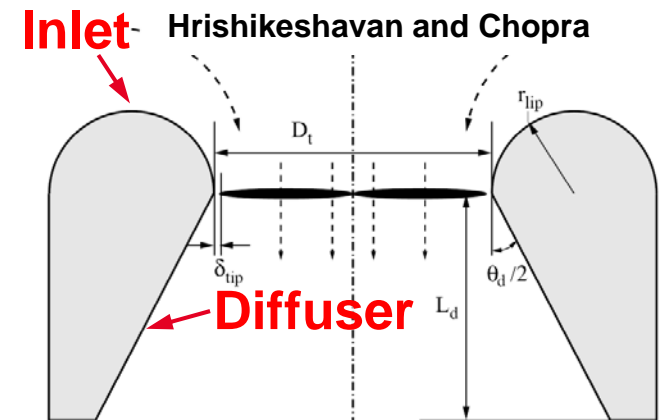
Shroud Configuration

- Throat diameter (D_t)
- Tip clearance (δ_{tip})
- Lip radius (r_{lip})
- Diffuser length (L_d)
- Diffuser angle (θ_d)
- Shape of outer portion of shroud not significant



Experimental setup

Hrishikeshavan and Chopra



Schematic of shroud



Micro-Scale Shrouded Rotor



Setup of Hrishikeshavan and Chopra

Rotor Configuration

- 2 bladed with 2:1 taper from 60%R
- Aspect Ratio of 4.84
 - 121mm radius and 25mm chord

Airfoil profile

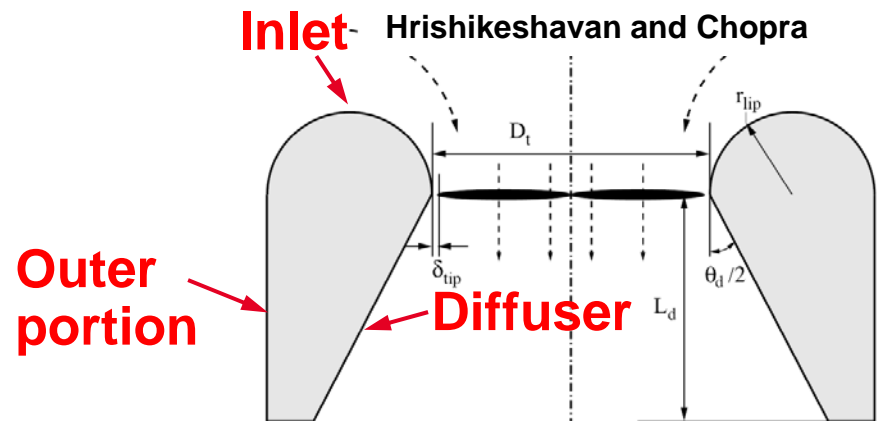
- Circular arc w/ LE sharpened from 8% chord
- 2% Thickness & 10% Camber

Shroud Configuration

- Throat diameter (D_t)
- Tip clearance (δ_{tip})
- Lip radius (r_{lip})
- Diffuser length (L_d)
- Diffuser angle (θ_d)
- Shape of outer portion of shroud not significant



Experimental setup
Hrishikeshavan and Chopra



Schematic of shroud



Micro-Scale Shrouded Rotor



Setup of Hrishikeshavan and Chopra

Rotor Configuration

- 2 bladed with 2:1 taper from 60%R
- Aspect Ratio of 4.84
 - 121mm radius and 25mm chord

Airfoil profile

- Circular arc w/ LE sharpened from 8% chord
- 2% Thickness & 10% Camber

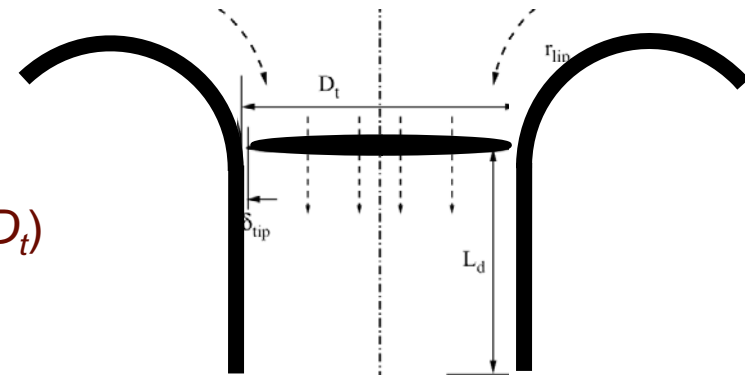
Shroud Configuration

- Throat diameter (D_t) → 247mm
- Tip clearance (δ_{tip}) → 2.5mm ($\sim 1\% D_t$)
- Lip radius (r_{lip}) → 9% D_t
- Diffuser length (L_d) → 15% D_t
- Diffuser angle (θ_d) → 0°
- Shape of outer portion of shroud not significant



Experimental setup

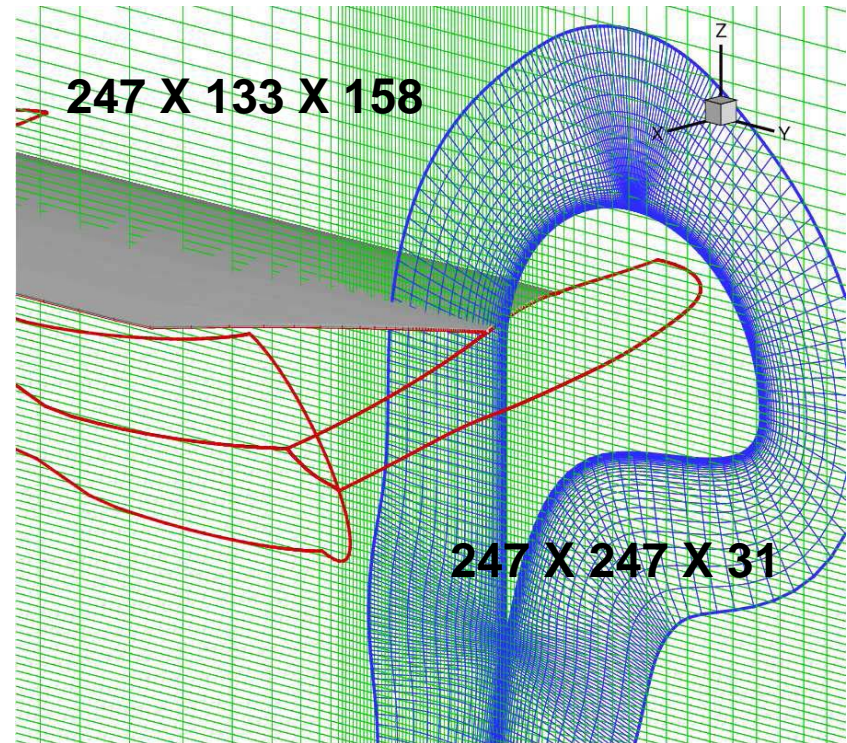
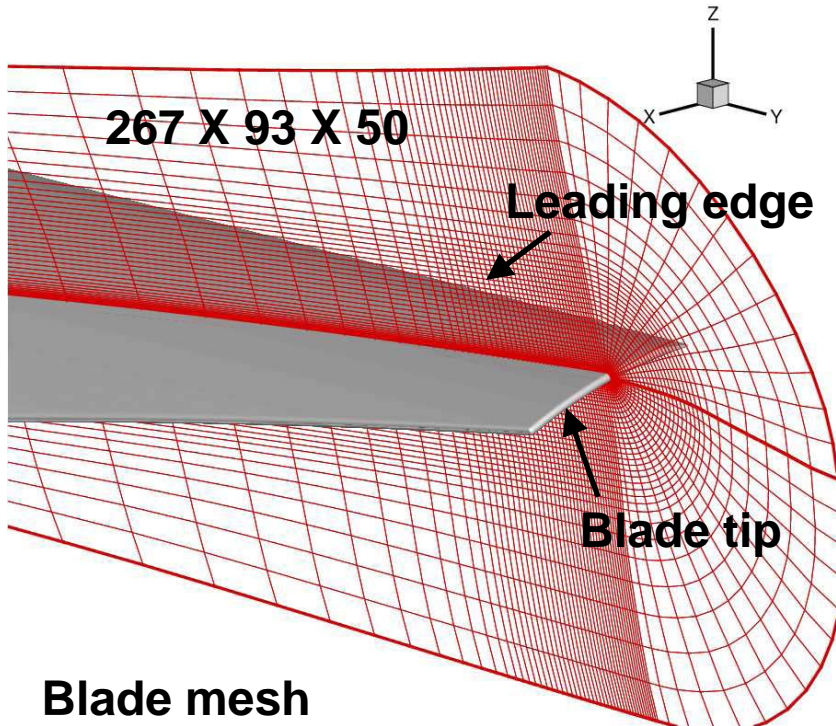
- Hrishikeshavan and Chopra



Schematic of shroud



Mesh System



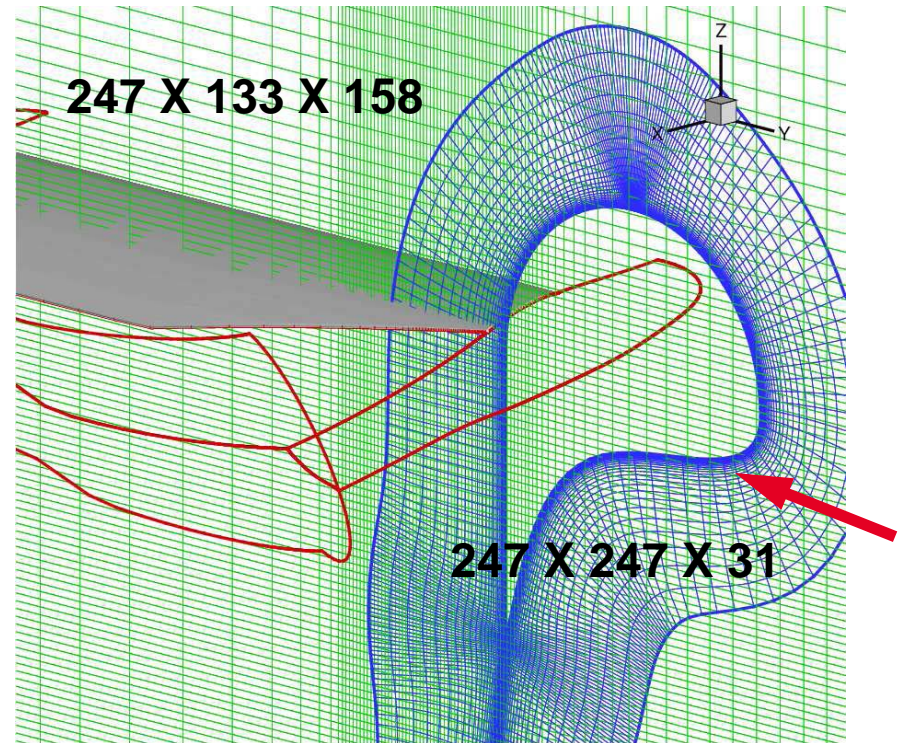
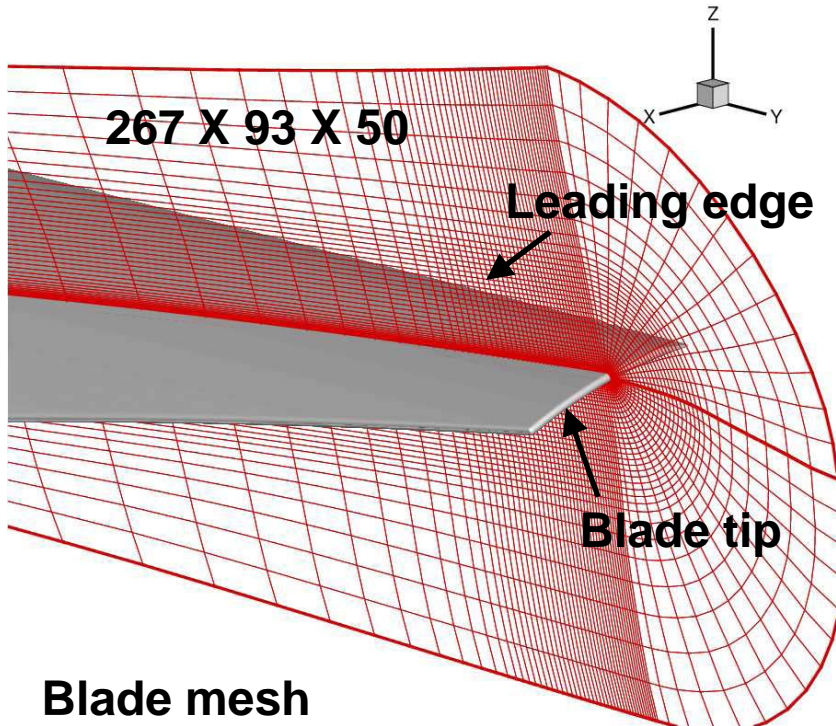
- Total mesh points ~ 10 million

- In most refined regions

→ $\Delta r = 0.025$ chords, $\Delta z = 0.04$ chords, $\Delta \psi = 1.5^\circ$, background



Mesh System



- Total mesh points ~ 10 million
- In most refined regions

→ $\Delta r = 0.025$ chords, $\Delta z = 0.04$ chords, $\Delta \psi = 1.5^\circ$, background

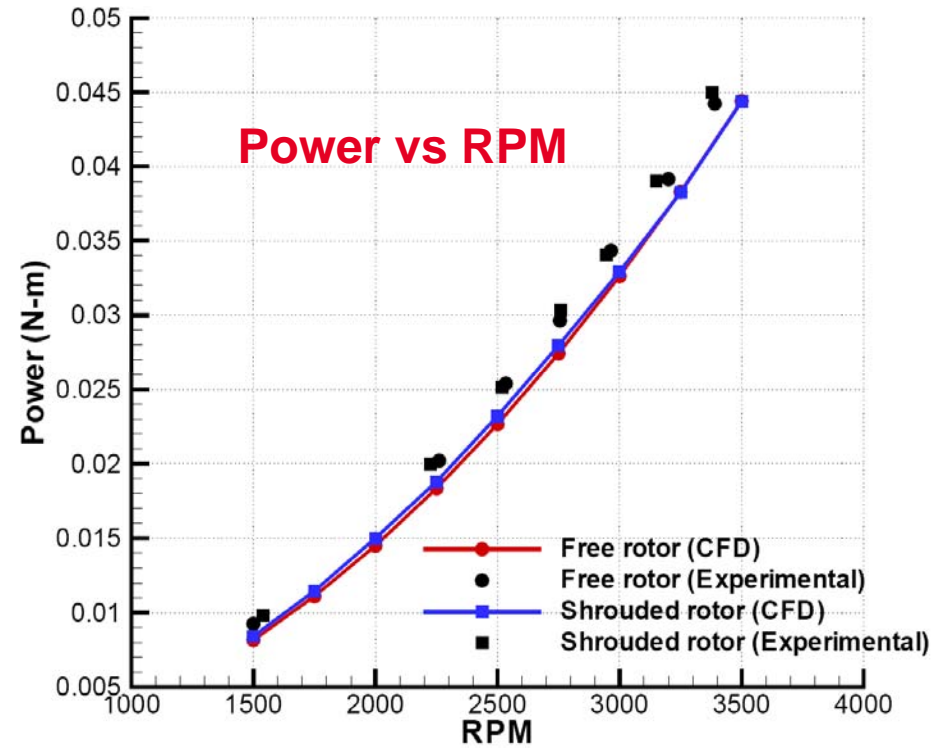
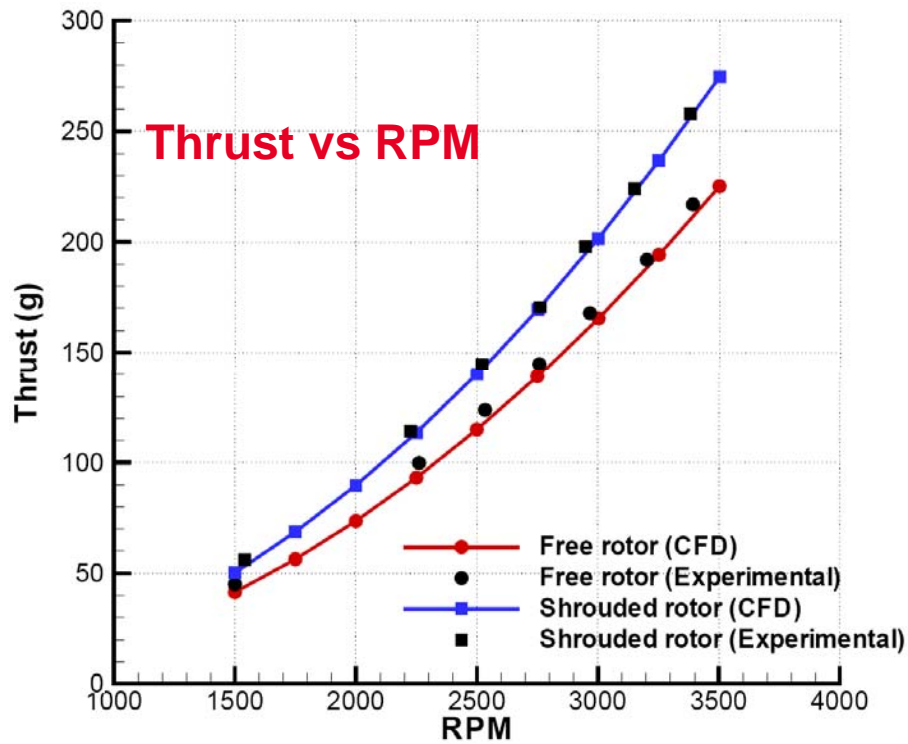
Outer portion of shroud closed to allow C-type mesh



Performance Comparison with Experiments



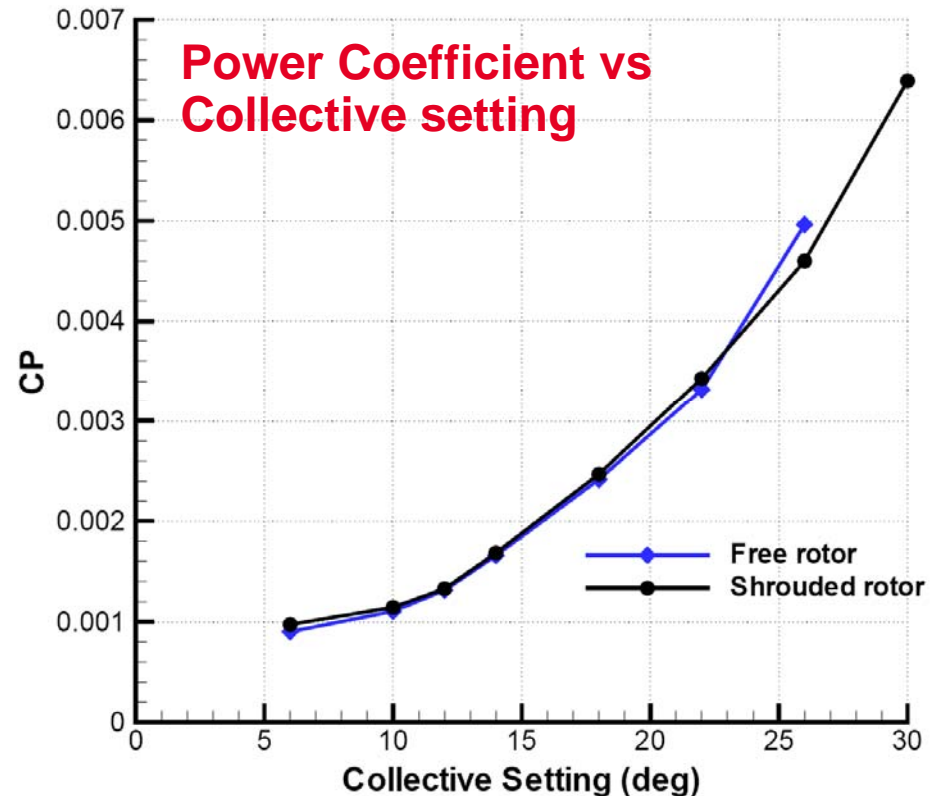
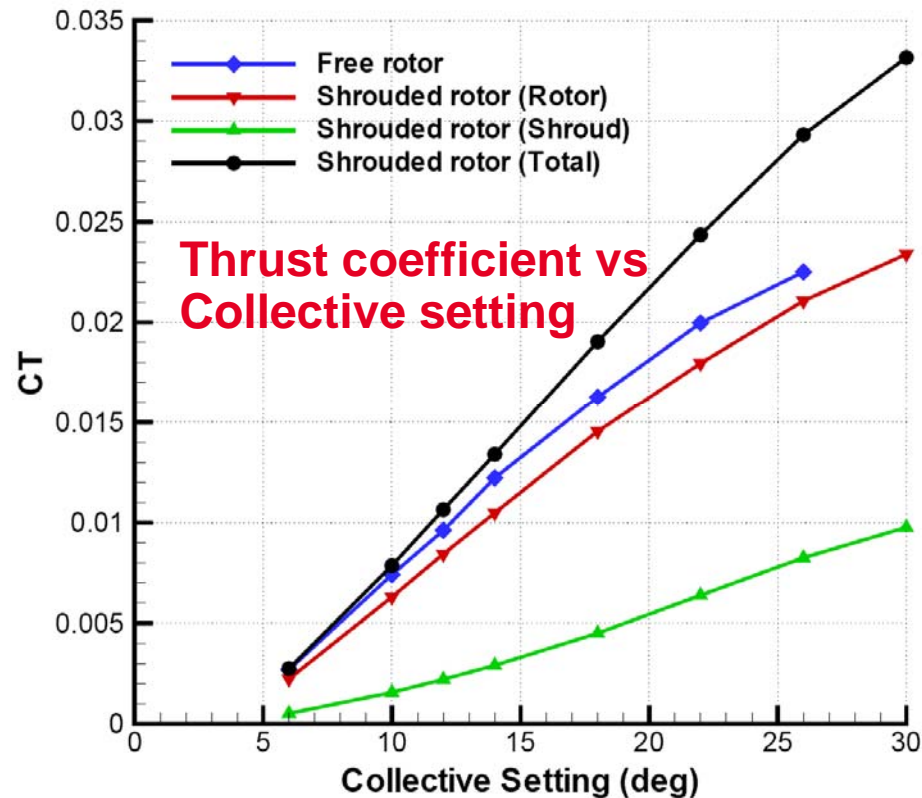
- Collective angle → 22°
- Tip Reynolds number → 30,000 to 70,000
- Tip Mach number → 0.056 to 0.131



Good comparison between CFD and experiment



Collective Angle Sweep (2500 RPM)

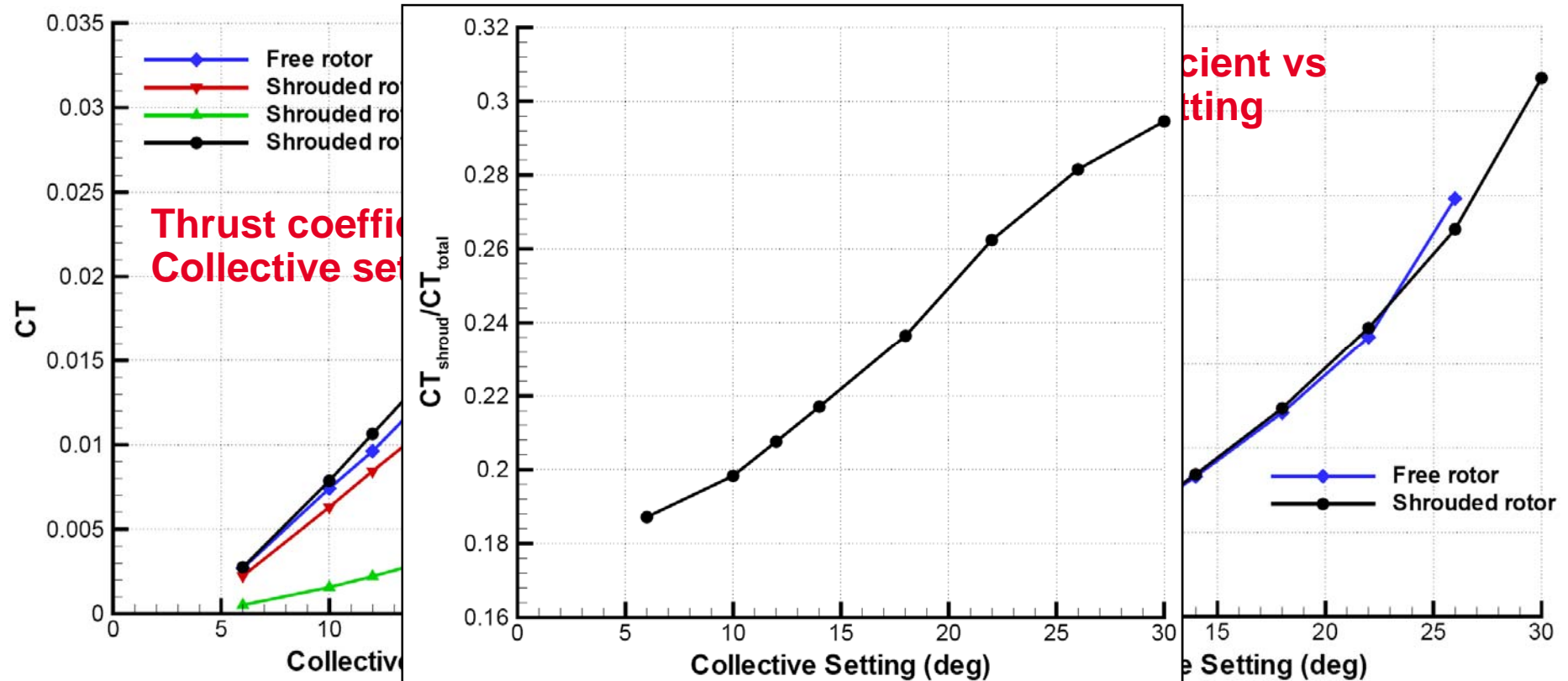


- **Shrouded rotor performance as compared to free rotor**

- ➔ Increased total thrust; decreased rotor thrust
- ➔ Almost Identical power



Collective Angle Sweep (2500 RPM)

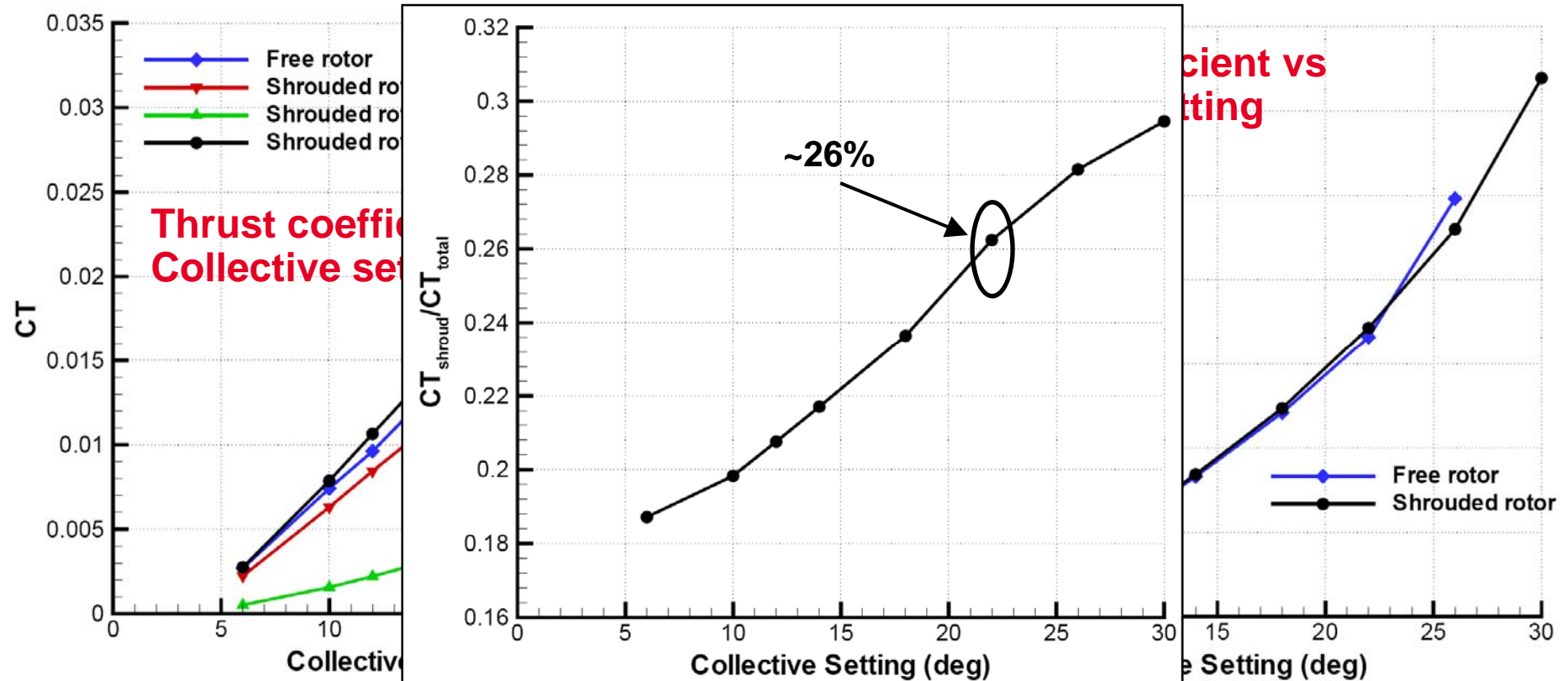


• Shrouded rotor performance as compared to free rotor

- Increased total thrust; decreased rotor thrust
- Almost Identical power



Collective Angle Sweep (2500 RPM)

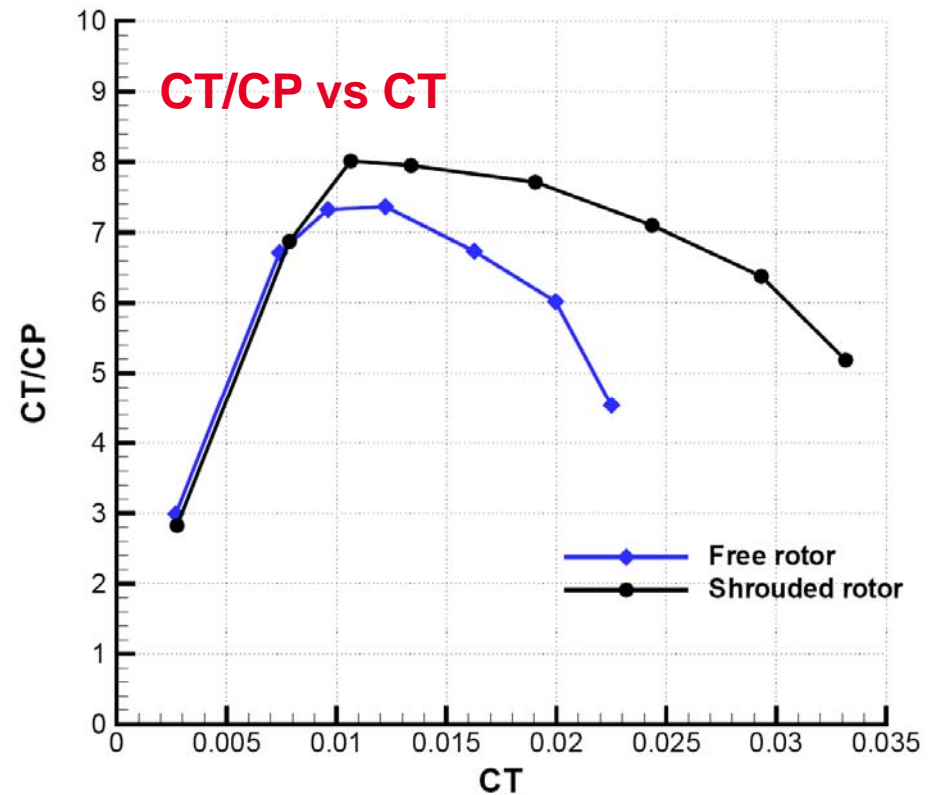
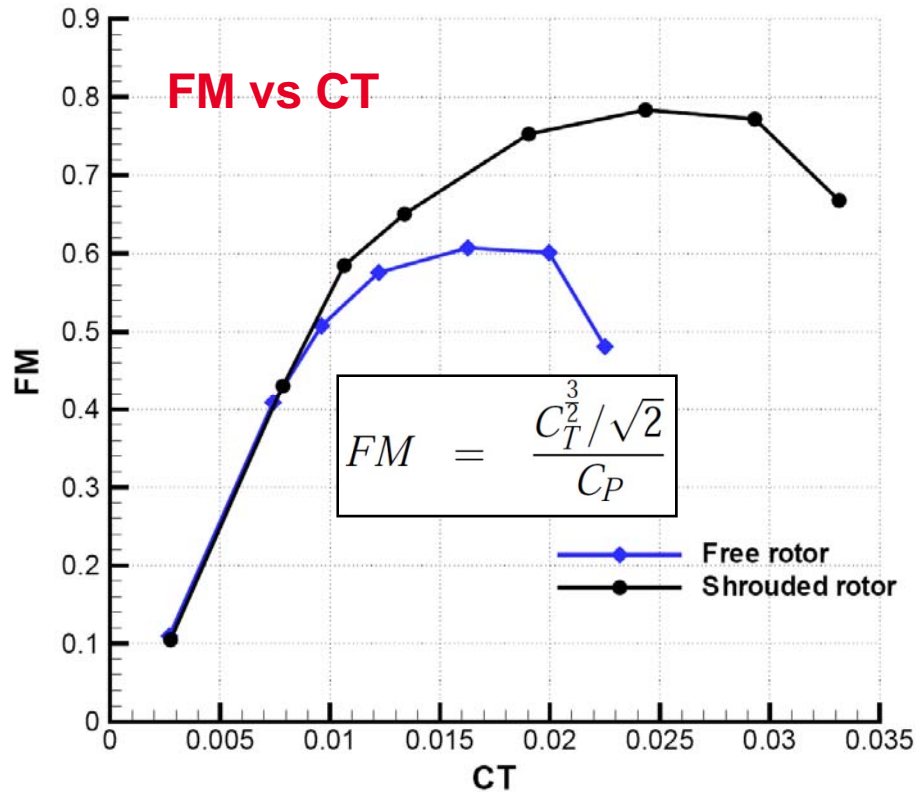


- **Shrouded rotor performance as compared to free rotor**

- ➔ Increased total thrust; decreased rotor thrust
- ➔ Almost Identical power



Collective Angle Sweep (2500 RPM) cont...

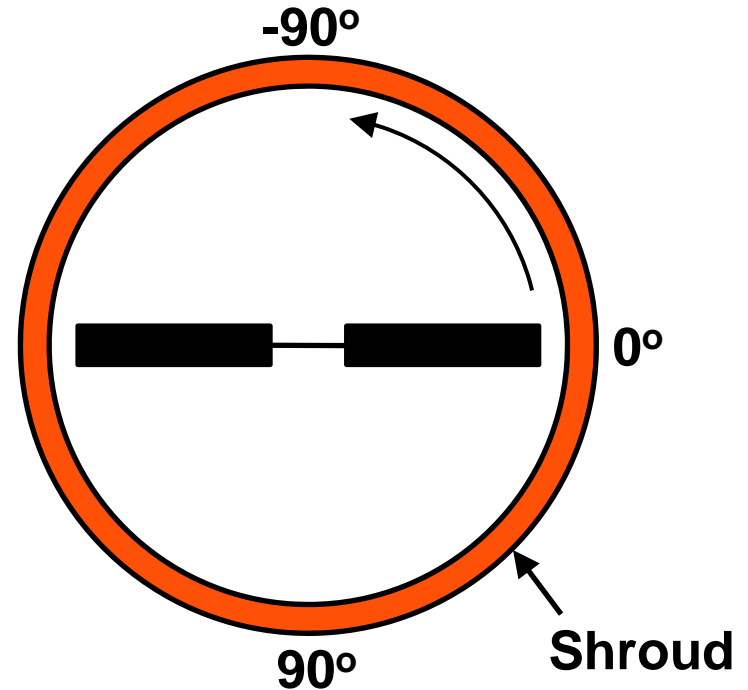
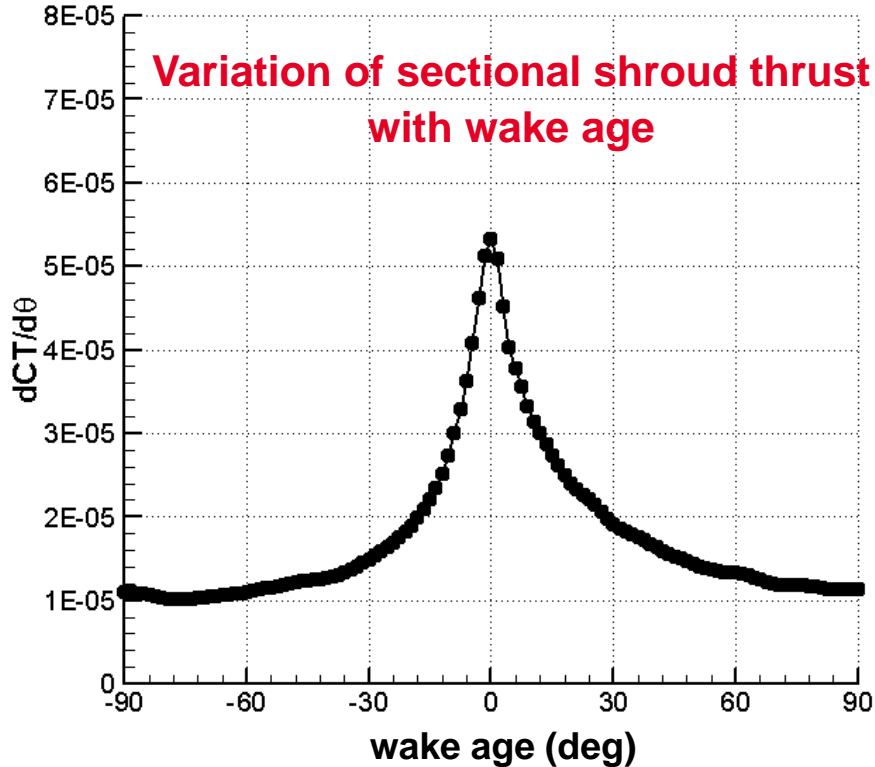


- Improved performance for shrouded rotor (~25%↑ in max FM)

- Peak FM achieved at higher thrust coefficient
- High FM and CT/CP for larger range of thrust coefficient



Shroud Performance (22° Collective Setting, 2500 RPM)

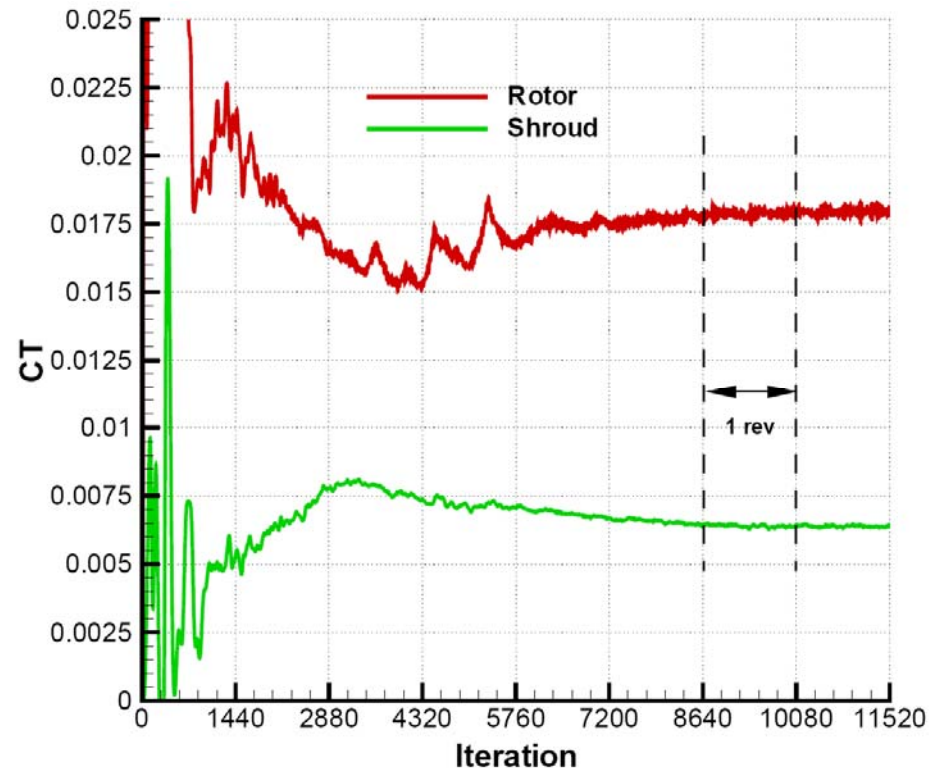
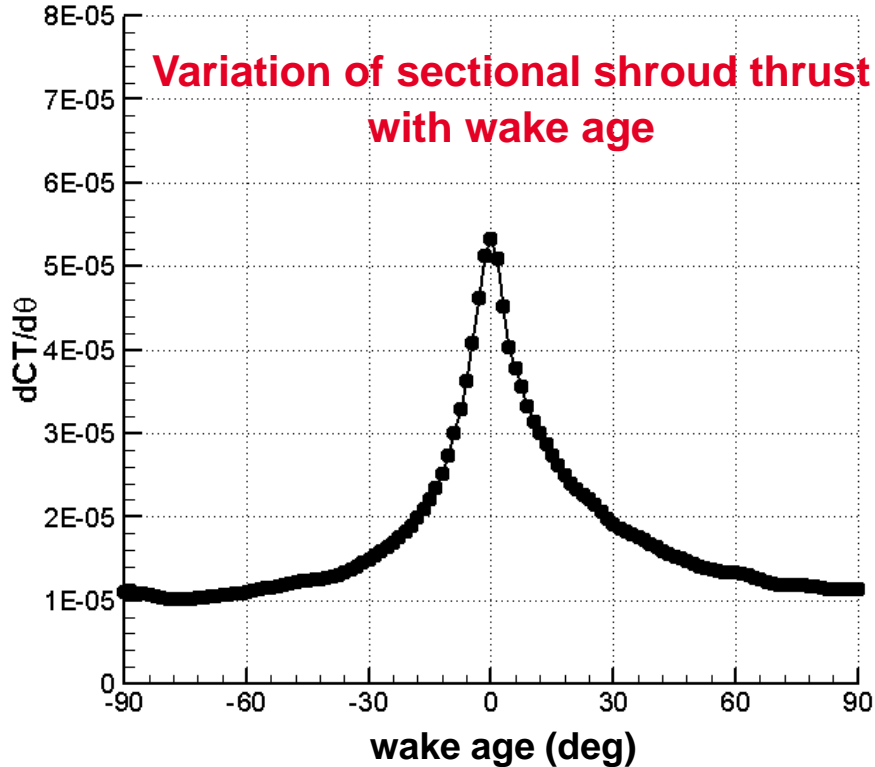


- **Shroud thrust**

→ Peaks near the blade position



Shroud Performance (22° Collective Setting, 2500 RPM)

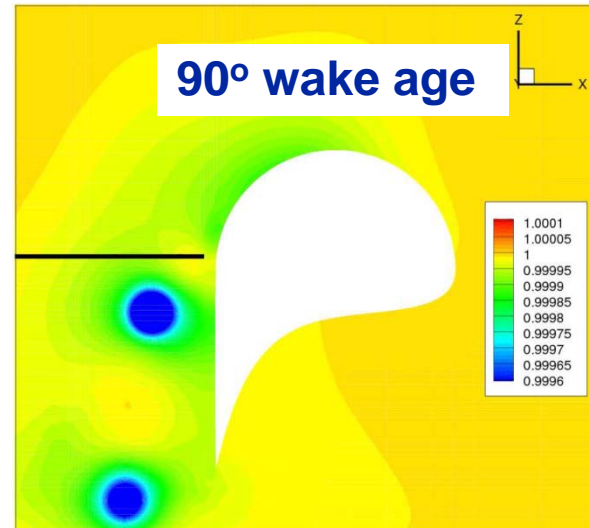
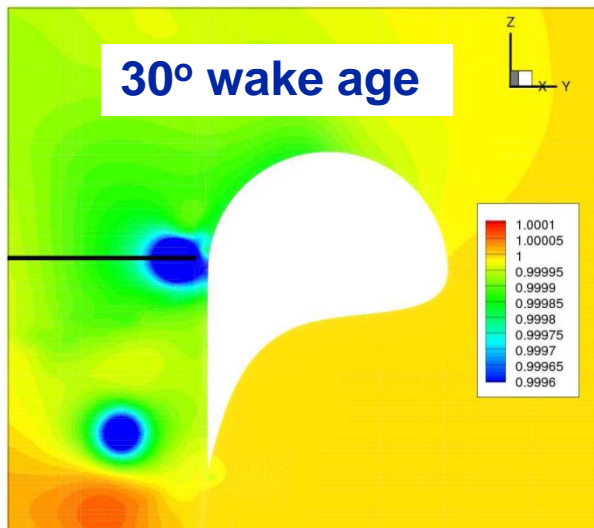
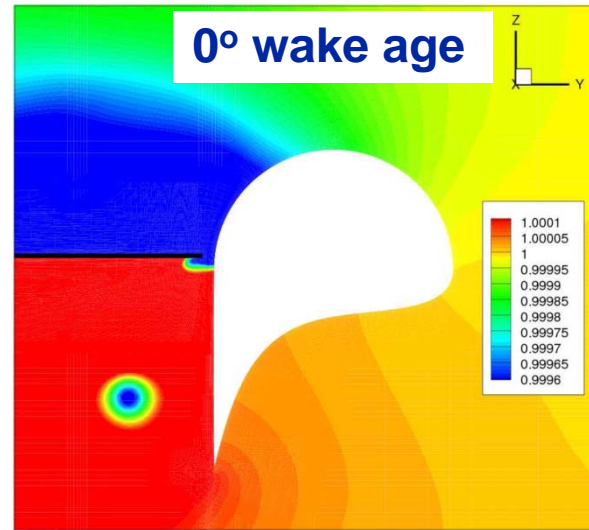
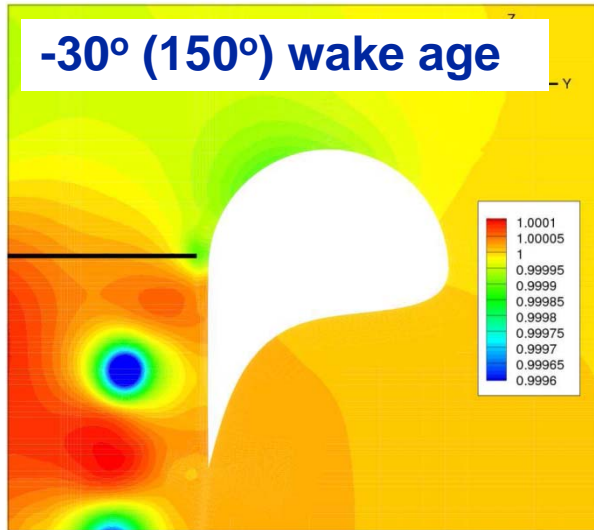


Convergence of rotor and shroud thrusts

Both rotor and shroud thrust remain fairly constant with time



Sectional Pressure Contour (22° Collective Setting, 2500 RPM)

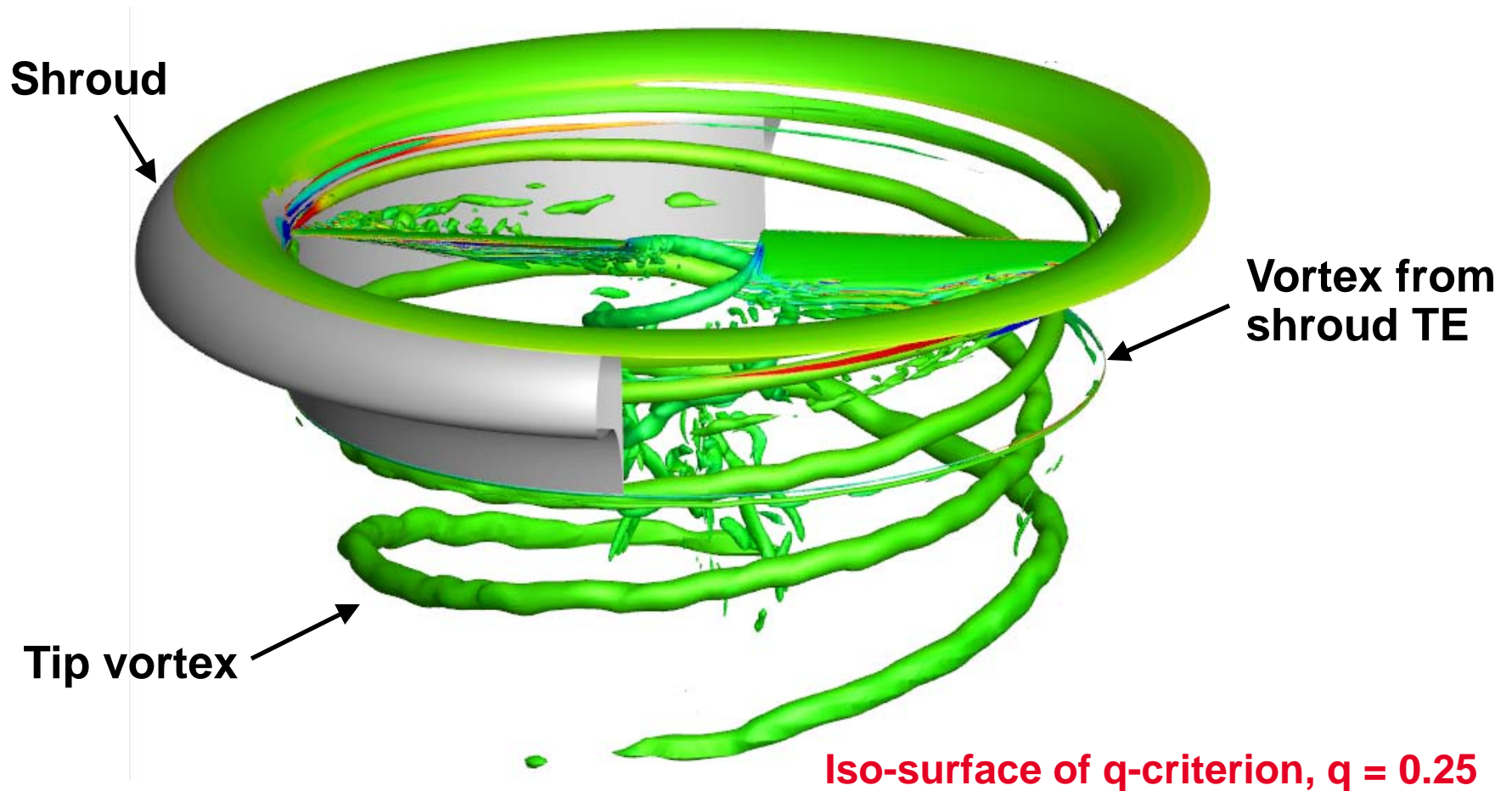


Two thrust producing mechanisms

- Low pressure created by blade acting on shroud
- Flow acceleration around shroud inlet producing low pressure
 - Accelerated by tip vortex



Flow Visualization (22° Collective Setting, 2500 RPM)



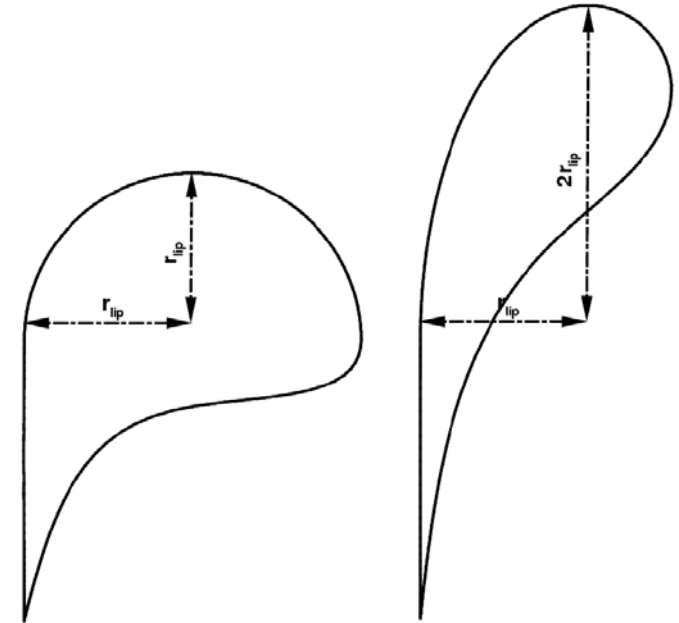


Proposed New Shroud Design



- **Proposed modified shroud which is more aerodynamic from a detailed shroud parametric study**

- ➔ Inner portion of inlet modified to 2:1 ellipse
- ➔ At leading edge, ellipse transformed to circle with identical radius
- ➔ Spline fit to close the trailing edge

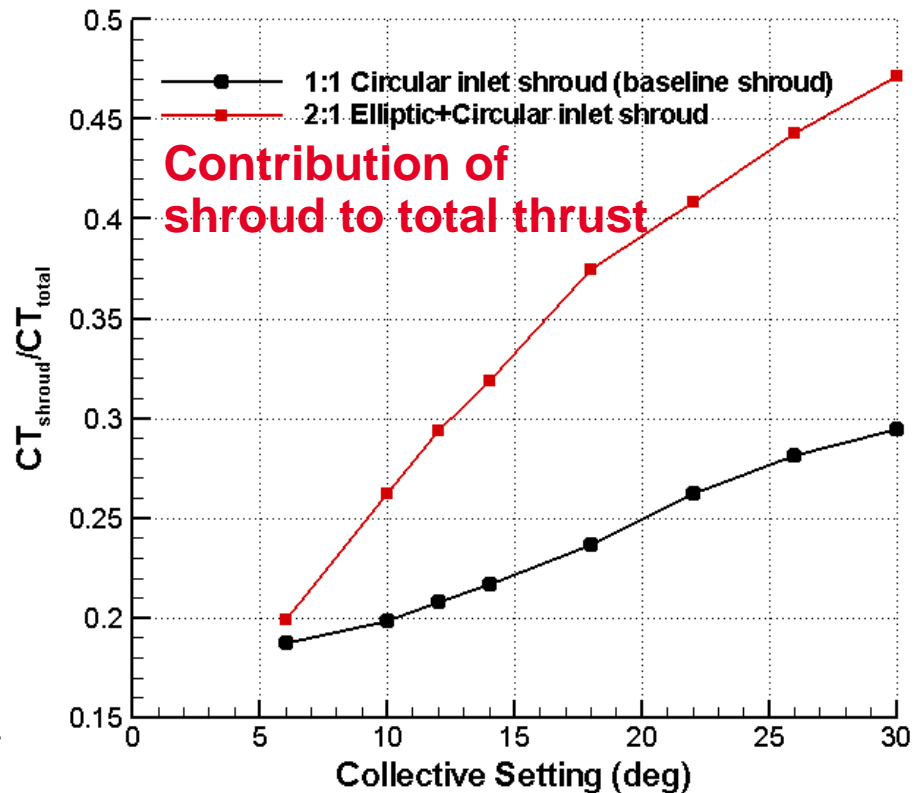
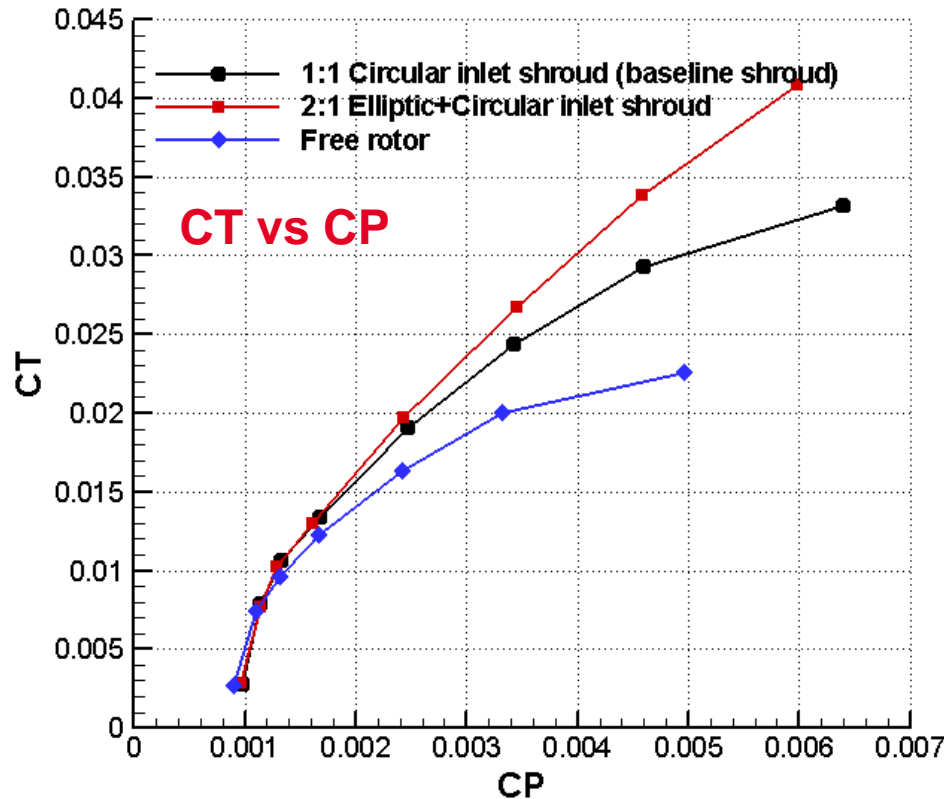


Original Shroud

**2:1 Elliptic+Circular
Inlet Shroud**



Modified Elliptic Inlet Shroud (Collective Angle Sweep, 2500 RPM)



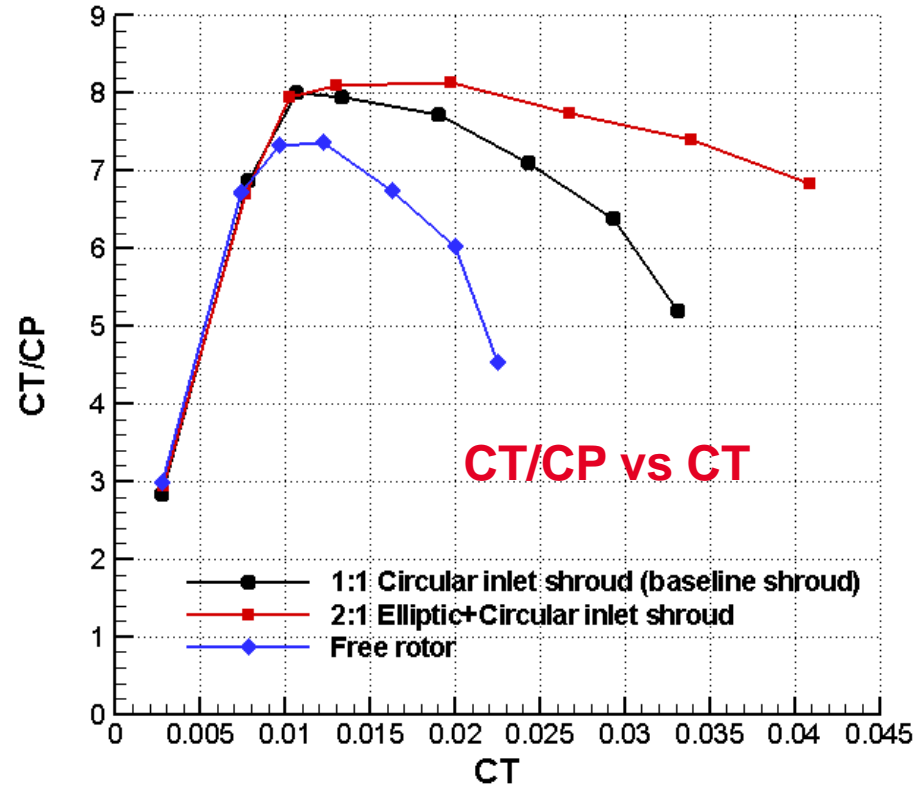
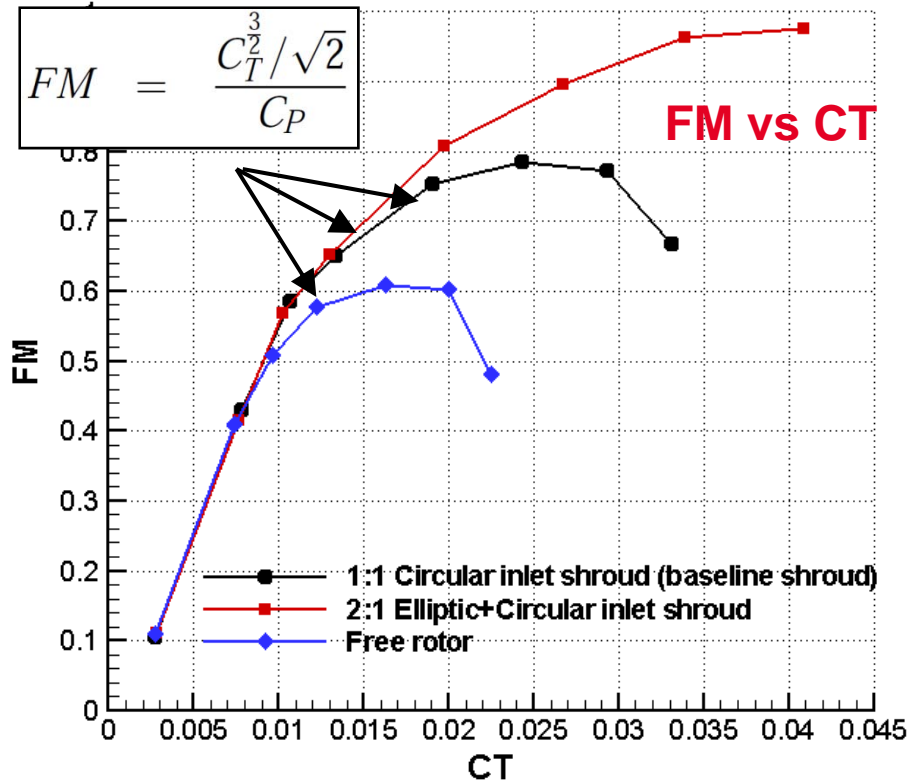
- **Improved performance for elliptic inlet shrouded rotor**

- ➔ Increase in thrust; Similar power

- ➔ Shroud contribution significantly higher (48% at highest collective angle)



Modified Elliptic Inlet Shroud (Collective Angle Sweep, 2500 RPM) cont...

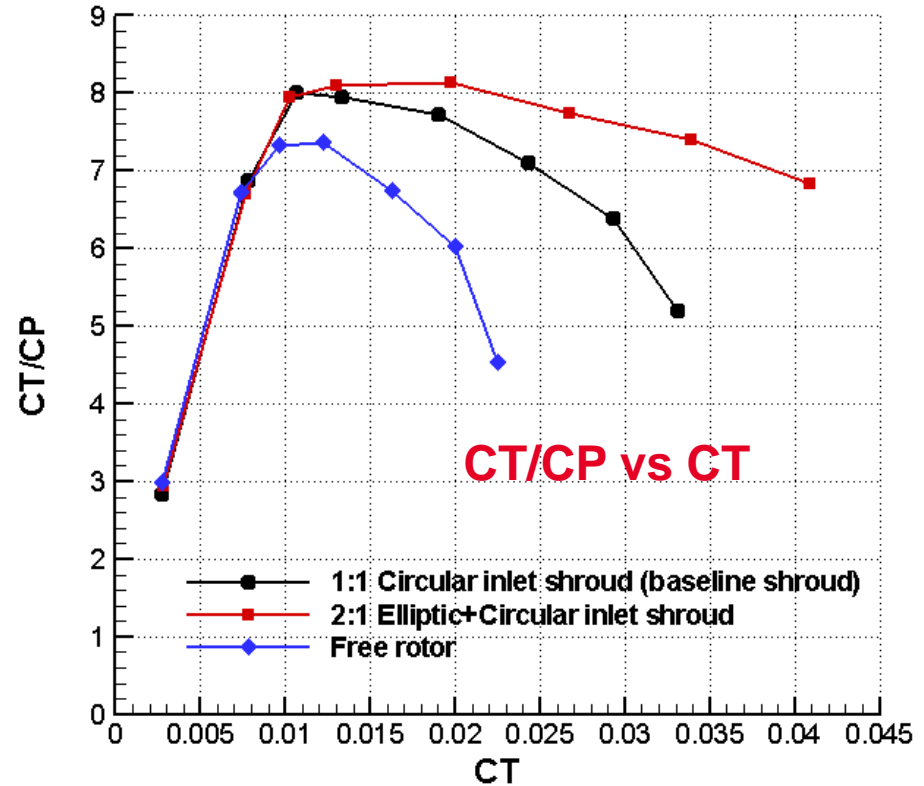
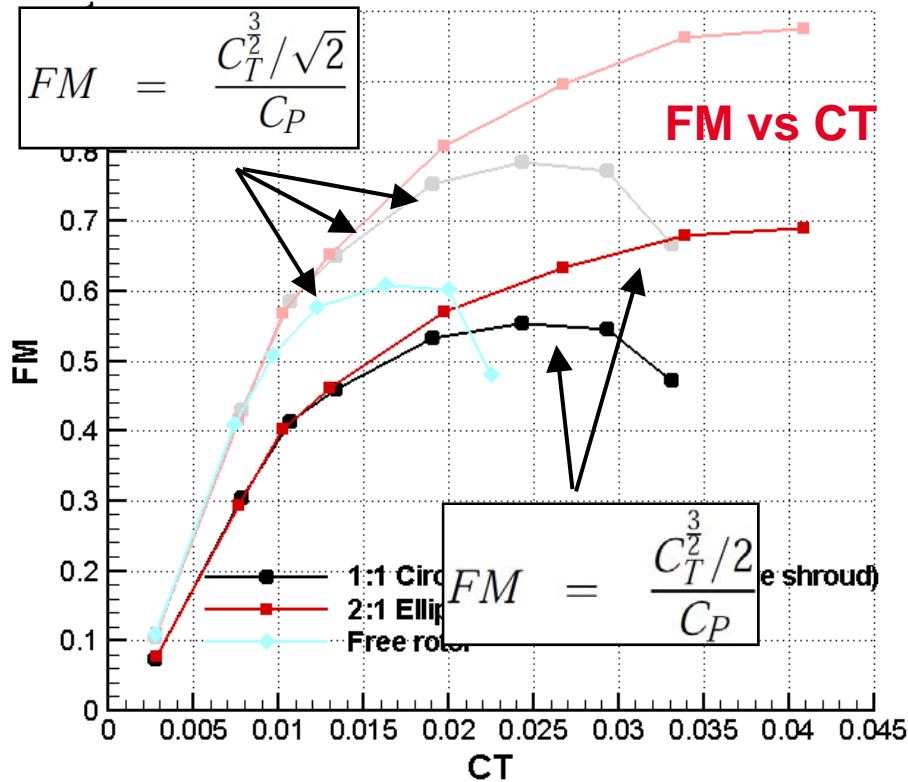


- Improved performance for elliptic inlet shroud configuration compared to baseline shrouded rotor (~25%↑ in max FM)

- ➔ Peak FM achieved at higher thrust coefficient
- ➔ High FM and CT/CP for larger range of thrust coefficient



Modified Elliptic Inlet Shroud (Collective Angle Sweep, 2500 RPM) cont...



- Improved performance for elliptic inlet shroud configuration compared to baseline shrouded rotor (~25%↑ in max FM)

→ Peak FM achieved at higher thrust coefficient

→ High FM and CT/CP for larger range of thrust coefficient



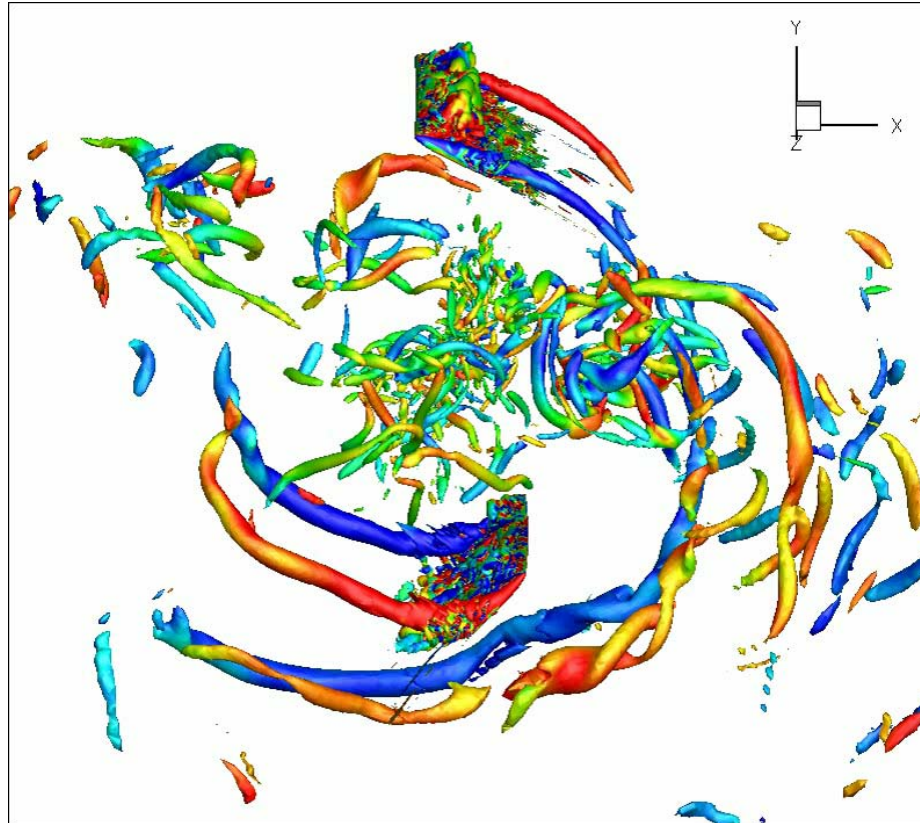
Summary



- **Improved Implicit Hole-Cutting (IHC) method by introducing new blanking technique**
 - ➔ New blanking technique applicable even to traditional hole-cutting method
- **Performed complex micro-hovering rotor calculations using overset grids and validated the results with available experimental data**
 - ➔ **Micro-scale single rotor:** Setup of Ramasamy et al.
 - ➔ **Micro-scale single rotor in IGE:** Setup of Lee et al.
 - ➔ **Micro-scale coaxial rotor:** Setup of Bohorquez and Pines
 - ➔ **Micro-scale shrouded rotor:** Setup of Hrishikeshavan and Chopra
 - ➔ **Micro-scale cycloidal rotor:** Setup of Benedict et al. (not shown)
- **Provided insight into the flow physics of various configurations**



Questions?



Flow visualization from Cycloidal Rotor simulation